Microwave Research Institute
Polytechnic Institute of Brooklyn
55 Johnson Street
Brooklyn 1, New York

Report R-276-52, PIB-215
Project Destination NR-075-215

The Use of Magnetic Amplifiers to Drive Two-Phase Servo Motors

by

M.J. Kabrisky

Title Page
Acknowledgement
Abstract
Table of Contents
35 Pages of Text
Appendix I (2 pages)
Appendix II (1 page)
Appendix III (2 pages)
Appendix IV (5 pages)
31 Pages of Figures

Contract Nonr-292(00)

Brooklyn 1, New York
July 28, 1952

ACKNOWLEDGEMENT

The author would like to thank all of those people who have been helpful during the fellowship period: the staff of technicans at the Microwave Research Institute which constructed and maintained a large part of the experimental equipment that was used; the other Research Fellows who worked on the magnetic amplifier project, whose discussions proved to be a helpful source of information and mental stimulation and to Mr. Joseph Reed who, at this writing is working on his doctorate diseratation of topics related to those in this thesis and who was of considerable assistance in planning the tack of this work.

The author would particularly like to acknowledge the help and guidance of Doctor E.J. Smith, and Doctor M.M. Liwschitz-Garik whose regular conferences were of great importance in guiding this work.

ABSTRACT

The purpose of this report is to consider the use of magnetic amplifiers to operate two-phase servo motors. The effects of the interaction between the motor and amplifier have been considered and these results are set down in the final section.

Several types of magnetic amplifier circuits have been investigated with regard to bias adjustment and external characteristics. Wherever possible, the amplifier has been viewed as a "black box", and an attempt has been made to justify a functional transfer-type description of the amplifier behavior.

Similarly, the motor is viewed externally as two terminals and a shaft protruding from a black box. A method of calculating the complete family of speed-torque characteristics is presented which requires only two easily performed measurements to obtain the necessary data. In addition, a new equivalent circuit for the motor is proposed which considers the motor as an equivalent speed or torque generator and enables easy computation of system performance.

The results presented here are based on data obtained from two different sets of four, matched, tape-wound, Hipernik V cores and a Diehl FPE 25-11 servo motor. It has been necessary to make some conclusions based on experimental results, the equipment used, however, is typical of that commercially employed and most of the results can probably be extended to cover other similar applications without additional theoretical vertification.

In addition to the main body of the report, there is incorporated an appendix which describes some of the unusual measurement procedures which were necessary in this work.

Table of Contents

I. Introduction

The history of the magnetic amplifier is too well known to be repeated here.[1] This report considers the use of magnetic amplifiers as sources of power for miniature two phase induction motors in instrument or computor servo systems.

The simplest form of a magnetic amplifier, electric motor servo system is shown in Fig. MRI-12648. The basically nonlinear links in the system are the motor and magnetic amplifier. Both devices are nonlinear "magnetic circuits", and indeed the operation of the amplifier depends on this very nonlinearity. This report, however, will point out certain linear viewpoints that may be taken regarding their external performances which will enable easy system calculations.

In the servo system shown, the performance of the mechanical load is observed by some form of electromechanical transducer which converts the pertinent aspect of load performance into an electrical equivalence. This electrical signal is then utilized as part of the total signal applied to the entire system.

II. The Magnetic Amplifier

A. Normal Transfer Curves

It will be shown later that the magnitude of the input impedance of the controlled phase of the two phase servo motor varies by approximately 15% about a fixed mean value over the entire range of motor operation and less than this in the usual range where the motor is operated. This extremely small variation is due to the very large magnetizing current drawn by the machine as will be seen later. Such a load on a magnetic amplifier, or for that matter any power amplifier, can be considered to be almost constant, especially if the load impedance is substantially higher than the source impedance as is frequently the case in these applications. As a result of this, it is possible to represent the magnetic amplifier as a two dimensioned transfer curve (output voltage versus the control quantity).

Fig. MRI-12649 shows a typical transfer curve of a sensitive material magnetic amplifier. This curve is that of a doubler type circuit and shows the RMS value of the 60 cycle component of the output voltage across a fixed load versus the control current. The ordinate might also represent DC output voltage, in the case of those circuits which produce such voltage, or even RMS output voltage. In other words, the type of transfer curve shown in Fig. MRI-12649 is representative of a great many types of magnetic amplifier circuits. Several of these circuits are shown in Fig. MRI-12650.

---

[1] For a complete bibliography of the magnetic amplifier see: Miles, James G., Bibliography of Magnetic Amplifier Devices and the Saturable Reactor Art. Proc. AIEE, Vol. 70, 1951.

It will be noted that the amplifiers are useful over only a limited range of control current variation. This, of course, is no particular disadvantage; a similar situation exists in the case of almost all electrical control devices. In their useful range, magnetic amplifiers using sensitive materials have fairly straight transfer curves. By suitable biasing, the entire curve may be transported, to the left or to the right parallel to the abscissa without change in shape.[2] For those circuits which produce DC output voltage, only one polarity of the output voltage is available. Correspondingly, for the AC output voltage circuits, phase reversal of the output is impossible.

For almost all servo applications, however, a reversal of output voltage is required, i.e. a DC voltage which can reverse polarity, or an AC voltage which can reverse phase. Usually, the output voltage is required to reverse as the input quantity reverses. Such reversable output circuits[3] are generally called "push-pull" amplifiers (not to be confused with electronic-type push-pull amplifiers).

B. Push-Pull Magnetic Amplifiers

Fig. MRI-12651 shows two full wave circuits connected to substract their DC output voltages. When cores A_1 and A_2 are completely saturated and B_1 and B_2 unsaturated, the output polarity from a to b is opposite that when cores B_1 and B_2 are saturated and A_1 and A_2 are unsaturated. As the control is varied, one situation blends into the other. In particular, when the outputs from both circuits are the same, the net output between a and b is zero. This situation may be representated by the curves in Fig. MRI-12652 where two identical transfer curves are shown producing a net voltage which is the difference between the output voltages of the indivual circuits. Note that the designation of one circuit or the other as producing "negative output" or the "positive output" is quite arbitrary.

As pointed out previously, the transfer curve of the indivual circuits may be easily moved along the abscissa; thus the overall transfer curve, the difference between the two indivual transfer curves, can be shaped rather readily. Some examples of this will be seen later.

An example of a circuit which produces reversable phase AC output voltage, is shown in Fig. MRI-12653. Here two doublers are arranged to subtract their AC outputs. When each doubler develops an equal voltage across its respective load resistor, there is no net output voltage. Should the balance be upset by varying the control current, there is a net output voltage of one phase or of the opposite

---

[2] If the connection of bias windings changes the restrained case to the free case, there will be some modification in the shape of the transfer curve.

[3] For a fairly complete discussion of reversable output magneic amplifiers see: Geyger, W.A., Magnetic Amplifiers of the Balance Detector Type-Their Basic Principles, Characteristics, and Applications, Proc. AIEE Vol. 70, 195.

phase, depending which doubler develops the larger output voltage. A convenient representation of this mode of operation is shown in Fig. MRI-12654.

Here a word of caution must be inserted. The overall output voltage curve is not the algebraic difference between the individual curves, since the AC output of each doubler consists of truncated sine waves. It is an unwarranted assumption to state that any component (fundamental, RMS, etc.) of such a resultant curve could be obtained by simple point by point subtraction of the two original doubler curves. An example of actual push-pull characteristics will be shown later.

C. Push-Pull Circuits Applicable for the Control to Two Phase Servo Motors

If a push-pull circuit is to be used to drive a two phase motor in either direction, it must be capable of delivering full output voltage of reversable phase. In the transition between full output voltage of one phase, and full output voltage of the other phase, the fundamental component of the output will, in general, stray from perfect quadrature with respect to the voltage applied to the controlled phase. It can be shown that the output torque at a specified speed is approximately proportional to the sine of the phase angle between the voltages applied to the two motor windings.[4] More will be said of this later in Section IV.

There are quite a few types of circuits which can produce reversable phase AC voltage.[5] Most of these are subtraction arrangements of the more familiar types of magnetic amplifier circuits which may utilize either external feedback or self-saturation-type feedback. The various push-pull circuits subtract either their output voltages or their output currents, so that one may speak of "voltage subtraction" or "current subtraction" push-pull amplifiers. As an example of a voltage subtraction circuit is shown in Fig. MRI-12655. For an infinite external load resistance across the split resistor output network, the two doublers are completely isolated from each other. As an external two-terminal load is applied, part of the current in one doubler circuit flows through the other doubler circuit. Fig. MRI-12656a, on the other hand, shows a push-pull amplifier which essentially subtracts the output currents of two doublers leaving a net output current in a common load. Both types of push-pull circuits are applicable to the operation of two phase motors, each type possess certain advantages and disadvantages.

---

[4] See Steinhacker, M.A., and Meserve, W.E., Two Phase A.C. Servo Motor Operation With Varying Phase Angle of the Control Winding Applied Voltage. AIEE Technical Paper 51-386, August, 1951

[5] See Cohen, op. cit. Geyger, op. cit. and Milnes, Magnetic Amplifiers, Journal of the Institution of Electrical Engineers, Vol. 95, Part I, No. 99, May 1949, pp. 89-98.

(1) The problem of the split load in voltage subtraction circuits

Voltage subtraction circuits require a split load as shown in Fig. MRI-12653. For applications where the actual useful load is split, such as a two field motor or relay, this is no problem. Actually it is a desirable feature. When the load is a two-terminal network, it must be connected across the extremities of a split network which is not a useful load.[6] This type of arrangement involves a rather large loss of power in the mixing resistors. An obvious remedy, would be to replace the split load resistor by a split transformer and place the load on a secondary winding. While this is a perfectly satisfactory circuit, a little reflection soon reveals that such an arrangement is equivalent to the current subtraction circuit whose attendant problems will be discussed shortly.

(2) The problem of circulating current in current subtraction circuits

One of the major problems in current subtraction circuits is the stray component of current that flows around the outside loop through both doublers and the supply transformer, by passing the load. When both doublers are saturated, the transformer voltage is impresses across the forward resistance of the rectifiers and the resistance of the windings of the saturated reactors. These resistances are usually much lower than the load resistance and very large circulating currents can flow. Such current serves no purpose as far as useful power is concerned and represents a complete waste. The waste, however, may be minimized with proper biasing of the amplifiers. Circulating currents are unavoidable in practical operation and may even be desirable under certain circumstances.

(3) Biasing of push-pull amplifiers

Figures MRI-12658a through MRI-12658e show the results of various bias currents in a push-pull amplifier in terms of relative position of the individual transfer curves and the push-pull doublers using the cores of set 1 as described in Appendix I. The unusual methods necessary for obtaining these oscillographic displays of transfor curves have been enumerated in Appendix I.

Fig. MRI-12656b shows the transfer curve of one doubler with no bias mmf, as obtained by the oscillographic technique. Note that, at zero control mmf, full output is obtained and that a negative control

[6] Recently, the Ford Instrument Company (Division of the Sperry Company) have made available a line of motors having two windings in both fields. This apparently was done for universality of applications considerations, but, of course, such a motor may be utilized as a split field device if operated at one-half of maximum ratings.

mmf, (of approximately .02 ampere-turns per inch) is required before the output voltage begins to diminish. Note, too, that there is a small hysteresis-type loop near the minimum point of the doubler. When traveling down the transfer curve; that is, going from maximum output voltage, the output changes smoothly, and by insensible degrees to the minimum output. However, when traveling in the opposite direction, the output voltage jumps abruptly. The jumps occurs when the control mmf has increased to an amount slightly more than was necessary to completely unsaturate the amplifier. Thus, near the minimum output point, the transfer curve is double valued. This is an unsatisfactory condition in most servo applications.

For ordinary doubler operation, the hysteresis loop may be eliminated by raising the AC supply voltage above the maximum voltage for which the doubler can remain completely unsaturated at the minimum point. Thus, the doubler must always saturate every cycle, if only very slightly; and the hysteresis jump never occurs. A similar treatment can be employed in the case of push-pull amplifiers.

Figures MRI-12657 through MRI-12658e show the relative positions of the respective doubler curves and the resultant push-pull characteristics for various amounts of bias mmf.

When two doublers with zero bias are connected in push-pull, their characteristics may be representated in Fig. MRI-12657. In this diagram, two transfer curves have been superposed, and the approximate over all transfer curve interpolated. The interpolation was necessary because actual operation of the respective transfer curves overlapping to such an extent (because of zero bias mmf) would cause enormous circulating currents (approximately 5 or 10 times full load current). As pointed out previously, such an algebric interpolation is not completely valid. Actually the results are fairly accurate especially if one is only interested in one component of the output, say the DC component or the fundamental component.

Figure MRI-12657 shows the impracticability of the zero bias arrangement aside from the circulating current disadvantage. Such an irregular transfer curve is seldom if ever, usable in feedback control systems.

Figure MRI-12658a shows the relative position of the two doubler curves with approximately .030 ampere per inch bias mmf. Note that the bias polarity on each doubler is such as to move the curves apart. With .030 ampere turns per inch bias, at zero control current, the output voltage for the indivdual doublers when not connected in push-pull is about 75% of the maximum. (It will be seen later, however, that there is a strong likelihood that the indivdual doubler curves shift upon completing the push-pull connection). At the zero output point, the circulating current is about

five times the actual load current. The upper push-pull curve is for mmf decreasing from nominal positive to nominal negative mmf, that is from right to left. (Note that due to the method of obtaining these curves they do not cross the abscissa as do the curves in Figures MRI-12654 and MRI-12657, but are folded at the abscissa, and after reaching the zero output point, proceed to a maximum on the same side of the abscissa). Both curves are the same so that the output voltage of the push-pull circuit is everywhere a single valued function of the control mmf. Since the bias mmf was sufficient to bring the usable portions of both transfer curves together so that they overlapped, an approximately straight and fairly steep push-pull characteristic was obtained through the zero control mmf point. Incidently, the particular cores used were very well matched so that the push-pull output is almost exactly zero for zero control mmf. Fig. MRI-12658b shows the relative position of the doubler curves with the bias increased to .036 ampere turns per inch. With this bias, the output of each separate doubler is about 45% of maximum at the zero control mmf point. When connected as a push-pull amplifier, the circulating current is twice the maximum load current. The push-pull characteristic in this case is also single valued.

Since the usual high performance servo system will be frequently near the zero outpoint point, and since the maximum circulating current occurs at this point, it will be necessary to limit the maximum circulating current to approximately the same value as the average load current. Of course, actual duty cycles and performance data are required to make an intelligent choice concerning the maximum allowable circulating current. The case shown in Fig. MRI-12658c is probably closest to a practical adjustment of bias. Here, with a bias of .042 ampere turns per inch, the unconnected doubler curves overlap only slightly. At the zero output point, the circulating current is approximately equal to the maximum load current.

Figures MRI-12658d and MRI-12658e show impractical biasing situations. The oscillographs show the push-pull characteristics with bias values of .047 and .052 ampere turns per inch respectively. As can be seen, such biasing mmfs spread the indivdual doubler curves sufficiently to prevent any overlapping whatsoever. Therefore, the push-pull characteristics show a distinct split at the zero control point.

A very significant feature of Figures MRI-12658d and MRI-12658e is the reappearance of the hysteresis jumps. These jumps, characteristic of the individual doublers, were effectively "subtracted out" of the push-pull characteristic when the doubler characteristics overlapped. The actual reason for the disappearance of the hysteresis jumps will be discussed under Part F, "Removing Hysteresis Jumps From Push-Pull Characteristics".

D. Biasing Considerations

Fig. MRI-12659 shows the variation of the peak circulating current (which occurs at zero control mmf) as a function of bias mmf with the applied AC voltage to the push-pull amplifier as a parameter. These curves have been obtained using the cores in set 2. It can readily be seen that slight variations in bias can have a large effect on the magnitude of the peak circulating current. Until the bias becomes sufficiently small to allow an overlap of the individual doubler transfer curves, no circulating current results. Once they overlap the circulating current grows very rapidly with only slight reductions in the bias. This is a consequence of the very low impedance through the two saturated doublers across the AC supply.

It can be seen that if there is any circulating current at all, slight variations in the applied AC voltage have a fairly large effect on its magnitude. This occurs because the applied AC voltage has a considerable effect in selecting the firing angle of the individual doublers. As the AC voltage is increased, the doublers fire earlier in the cycle, hence, for a fixed bias, if there is circulating current, the magnitude of the circulating current will increase with an increase in the applied AC voltage. In addition to this effect, the instantaneous circulating current is directly proportional to the amplitude of the applied voltage.

Unfortunately, it is not possible to separate the circulating current from the load current except when the load current is zero. Fig. MRI-12661 shows a plot of the AC current (RMS) in one doubler as a function of control mmf for typical values of bias mmf and applied AC voltage (selecting these will be discussed later).

It is apparent that the variation of the peak circulating current with changes in both AC supply voltage and bias mmf is rather large. While the variation of peak circulating currents may be quite large, this has only a very slight effect on the external transfer curves as can be seen from Figures MRI-12658a through MRI-12658c. These curves are the push-pull characteristics of two doublers with bias variations of approximately 16% about a mean value of .037 ampere turns per inch; as can be seen the variation in the external characteristics is quite small, even though the maximum circulating current varies from five times the normal load current to about the same as the normal load current.

Of course, if the amplifier is not capable of supporting the heavy circulating currents occasioned by too little bias or too much supply voltage, such regions of supply excursion must be barred. But, withal, there is quite a large permisible variation of both bias and supply voltage - limited at one extreme by seperation of the doubler characteristics, with the attendant dead zone and hysteresis jumps, andat the other extreme by overly large circulating currents, or perhaps loss of gain at the zero control mmf point as the doubler curves overlap too far.

E. Power Handling Rating of Push-Pull Amplifier Components

1. Current Subtraction Circuits

If one considers a current subtraction circuit using two doublers it can be seen that for a load of W watts, the individual doublers must be of 2W watts capacity. For when one doubler is conducting fully and providing half of the secondary voltage to the load, and other doubler must be capable of remaining completely unsaturated for the entire cycle with full secondary voltage applied. It can be seen that for a load of W watts it is necessary to use a total aggregate of amplifiers that are capable of controlling 4W watts in their normal connection. This figure might be reduced to a certain extent if it is anticipated that the system will operate away from the zero load voltage (maximum circulating current) condition for most of the duty cycle and for approximately equal periods of time on each side of the zero output point. For ideal conditions of this sort, the capacity of the amplifier might be cut in half. Usually , however, high performance systems are expected to center, for most of the duty cycle, about the zero voltage point and the situation outlined above seldom obtains in practice. However, if the maximum circulating current is minimized by careful adjustment and accurate maintenance of bias and supply voltage, it would probably be possible to cut down somewhat, the figure of 4W watts.

2. Voltage Subtraction Circuits

The power handling requirements of the components making up a voltage subtraction amplifier or split load push-pull magnetic amplifier, cannot be stated as simply as in the case of the current subtraction circuit.

As previously alluded to, these circuits are most generally adapted to the excitation of electrically split electromechanical transducers such as two field motors. If such a load is to be used, it can be said, that except for circulating currents occasioned by stray coupling between the load halves (as might well be the case in a two field induction motor), and considering a duty cycle as outlined above, for a load of W watts, an aggregate of amplifiers comprising only W watts is required.

If the useful load is not electrically split, a dummy split load output network must be incorporated to perform the voltage subtraction. This is generally an undesirable procedure because such a network wastes power and occasions the use of larger than necessary magnetic amplifier components. It can be easily shown, for instance,

that in the circuit of Fig. MRI-12653, the source impedance seen by the useful load across terminals a and b approximetely equal to R, the impedance of one half of the split load. For a duty cycly employing both of the component amplifiers (comprising the push-pull amplifier) for one half the time, each amplifier must be capable of delivering 3W watts for an external useful load of W watts. This is because each amplifier must deliver 5W watts to the dummy load and W watts to the useful load for one half the time. Therefore, an ation of amplifiers of total power handling capacity of 6W must be employed. (This is not the optimum adjustment).

Usually an internal impedance comparable to the load impedance is undesirable, even in the case of the almost constant input impedance of the two phase servo motor. One consideration in this regard is the dynamic damping; the lower the source impedance, the greater is the motor damping and the less likelihood there is of single phase operation. Frequently, these considerations are of such importance that a high internal impedance may not be tolerable. The output impedance of a current subtraction circuits can be easily made much lower then that of voltage subtraction circuits. The impedance of such circuits is approximately the same as that of a single doubler.

F. Removal of Hysteresis Jumps from Push-Pull Characteristics

(1) Voltage Subtraction Circuits

Hysteresis jumps can be removed from voltage subtraction circuits by applying sufficient AC voltage to each of the component amplifiers, comprising the push-pull amplifier. Divesting both amplifiers of the jump, in the voltage subtraction circuit, precludes the possibility of the jumps appearing in the overall push-pull characteristic. Note that it is not at all sufficient to merely overlap the individual transfer cirves to prevent the jumps from appearing in the push-pull characteristics. If only this were done, the jumps would appear no matter how the curves were overlapped.

(2) Current Subtraction Circuits

Techniques to the above may be employed in the case of current subtraction push-pull circuits. Consider, for instance, the case of the doubler subtraction circuit of Fig. MRI-12656a. When one doubler conducts, the AC voltage which it applies to the load is at most, only one half of the maximum voltage which it can handle. At first glance, it would seem that the hysteresis jump is inevitable since

apparently, there is a minimum point for the individual doublers where only magnetizing current flows. If, however, care is taken in biasing so that the transfer curves of the individual doublers overlap past their respective hysteresis jumps, and if sufficient AC supply voltage is supplied to the push-pull amplifier, the jumps may be removed. For it will be noted, that the full AC supply voltage across the split transformer is applied to the doubler which is conducting only for a small period, somewhat before the time in each cycle when it is fired. Thsi occurs after the other doubler fires earlier in the cycle. Thus for part of each cycle the voltage applied to the lesser conducting doubler is twice the voltage ever seen by the load. If this voltage is high enough, (sufficient AC supply voltage) and if it is applied lonag enough (sufficient overlap), the effective minimum point for each doubler can be moved up past the magnetizing current value. In other words, it is possible to force each doubler to conduct every cycle. As a result the hysteresis jump can be avoided.

For the set of smaller cores (setII) used by the author (see Appendix I), it was found that an applied AC voltage of fifty volts across the full supply transformer and an overlap of characteristics permitting peak circulating currents of about the same order as the maximum load current insured the absence of the jumps. It is to be noted that the maximum voltage which the cores could handle and have one of the doublers completely cut off was about forty-two volts (each doubler could remain completely cut off with twenty-one volts applied).

The hysteresis problem seems to have only been scantily mentioned in the literature; therefore it is important, using a new push-pull circuit, to check very carefully for the existence of any jumps, since their existence in a feed-back system would prove detrimental. It is possible that techniques similar to those described previously can be used to eliminate hysteresis characteristics from other types of push-pull circuits when they occur.

G. Characteristics of the Push-Pull Transfer Curve as Regards Feedback Systems

When considering the use of push-pull magnetic amplifiers in feedback systems, it is important to consider not only the usable and sensitive range of the transfer curve, but also the fairly flat or "saturated" part of the transfer curve. For instance, Fig. MRI-12652 shows the individual amplifier characteristics and the resultant push-pull characteristics. In regard to the individual transfer curves, it can be seen that if the control current is increased negatively past that necessary to achieve minimum output, the output of

the individual amplifier once again begins to rise, though at a much lower rate. The effect of this rise can be seen in the composite push-pull curve where, past the sensitive control current. In a feedback loop, this means a phase reversal of 180 degrees in the loop-gain-transfer function. For this type of system, the circuit immediately becomes inoperative when the control current excursion exceeds the central portion of the transfer curve. The possibility of such a situation occuring is particularly great when servo systems are turned on or when subjected to heavy external mechanical loads or large electrical input signals. To avoid such a possibility, it is necessary to place somewhere in the system, a device which will saturate before the magnetic amplifier from ever reaching the saturated region.

H. Transient Consideration

For applications where the load on a push-pull amplifier is fairly constant, we have seen that the amplifier may be represented, for static considerations, by a two dimensioned transfer curve. This is a very convenient representation when the amplifier merely becomes one link in a system. For servo work, however, a dynamic transfer is a very valuable piece of knowledge and enables the design engineer to make intelligent predictions concerning the measures necessary to stabilize the system into which an element is incorporated. Several methods have been advanced in the past to describe the dynamic performance of magnetic amplifiers. One of the most common is the assumption of a simple RL transient taking place in the control circuit: the assumption being that the output of the amplifier follows the control current and that the finite time response of the magnetic amplifier is due only to the inductive lag in the control circuit which prevents the control current from changing instantly. The actual mechanism is known to be more complicated than this; in this regard it is only necessary to mention as one factor, that inductances comprising the control circuit reactance are nonlinear. The method, however, gives fairly good results for several types of circuits. The doubler is not one of these, though; the doubler, in fact, may demonstrat rates of decay and build-up for step inputs, which differ markedly from each other. There is no linear circuit which can approximate such performance.

III Two Phase Servo Motors

A. General Description

The term AC servo motor is usually taken to include that

peculiar type of AC induction motor which has a high torque-to-inertia figure of merit and approximately straight line speed-torque curves in the range of slip from zero to one. These machines are usually two-phase machines, because this type of induction motor may be designed to be reversable and yet exhibit complete control of speed and torque by the variation of only one input parameter. Typical manufacturer's data is shown in Fig. MRI-12662. This is usually the only data which manufacturers make available. Most servo motors have electrical characteristics very similar to those of Fig. MRI-12662. The principal characteristics of servo motors may be described as follows:

(1) Approximately straight line speed-torque characteristics, or at least two approximately straight line regions, one for high speeds, one for low speeds. This type of characteristic is obtained by making the reflected rotor resistance very large. As is well known,[7] increasing this resistance, moves the peak of the speed torque characteristic to the left in a diagram like that of Fig. MRI-12663. In the case of most servo motors this peak has been moved so far to the left, that maximum torque occurs at a slope of 1. Thus a fairly linear speed-torque curve can be obtained over the entire useful range of slip.

(2) An almost constant input impedance, resulting in an almost constant input current independent of speed. The impedance angle varies, however, as the motor extracts varying amounts of power from the source depending on the load requirements.

(3) Extremely low efficiency as evidenced by the large discrepency between input and output power in Fig. MRI-12662.

(4) In addition, Diehl motors are built to deliver approximately 63% of locked-rotor torque at 55% of synchronous speed, this is a rough measure of the departure from true linearity that the speed-torque curves take.

(5) These motors are rated by their maximum power output. The Diehl catalogue lists a great number of different motors with maximum power outputs ranging from .5 watts to 750 watts. Despite this wide range of variation, all of their electrical characteristics are very similar to those shown in Fig. MRI-12662. The motor used in this investigation is one such typical machine of four watts maximum output power.

Servo motors are usually operated with a fixed, or referenced voltage on one phase (winding) and a variable control voltage on the other phase. For a specified torque output, the speed may be varied, by varying the voltage on the control phase. The family which results is shown in Fig. MRI-12664. These curves were measured during the course of this investigation. (See Appendix III)

---

[7] See, for instance, Liwschitz-Garik and Whipple, Electric Machinery, Vol. II, Van Nostrand, New York City, 1946.

B. Physical Description

The external physical dimensions have been shown in Fig. MRI-12662. The rotor is comparatively long and thin in order to improve the torque-to-inertia figure of merit; for the particular machine used, the rotor diameter is 0.6205 inches and the length is 1.5 inches. The high rotor resistance is achieved by using cast aluminum rotor bars of small cross section; they are eleven in number, skewed 60 electrical degrees. The stator has only eight slots with a three slot coil pitch; the stator diameter is 0.6302 inches which leaves an 0.005 inch air gap. This is a very large air gap for a machine of such small dimensions, approximately four times as large as that usually found in [illegible]otors if all dimensions were scaled up to typical motor size. It represents, however, about the smallest gap mechanically feasible in a production unit. It is probable, that the machine would be built with such a large air gap, even if a smaller one could be provided conveniently. This is because it results in most of the magnetizing reactance occuring in the gap and, as a consequence, the machine never saturates when normal voltages are applied. Such a feature makes linear speed-torque curves possible over the entire operating range of the machine. In addition, the large air gap causes a very large magnetizing current to flow; the result is the almost constant input impedance independent of speed.

C. Electrical Performance of Two Phase Servo Motors

The data published by servo motor manufacturers usually comprises only that shown in Fig. MRI-12662. The most significant curve, as far as system design is concerned, is the speed-torque curve. This curve is usually given for balanced operation (equal voltages applied to both phases, in perfect quadrature) in the region from no load to stall. For accurate prediction of closed system performance a family of such curves such as the one shown in Fig. MRI-12664 is required. The curves are seldom, if ever, available from the manufacturer.[8] System designers, therefore, make the following assumptions:

(1) The slopes of the entire family of speed-torque curves are constant and given by that of the speed-torque curve for balanced operation as provided by the manufacturer.

(2) The output torque at a specified speed is directly proportional to the AC voltage applied to the control phase of the machine when the reference voltage is fixed.

---

[8] See Koopman, R.J.W., Operating Characteristics of TWO-PHASE SERVO MOTORS AIEE Transactions, Vol. 68, New York, N.Y., 1949.

(3) The speed at a specified torque is directly proportional to the AC voltage applied to the control phase, when the reference voltage is fixed.

As regards assumption (1), it will be noted from the family of speed-torque curves in Fig. MRI-12664, that for the FPE 25-11, at least, the speed-torque curve is not a straight line. Most two phase motors have this later type of characteristic, although some do indeed have an almost straight line speed-torque characteristic. It is to be observed, that the speed-torque curves of Fig. MRI-12664 can be approximated quite well by two straight line regions as shown in Fig. MRI-12665. Fig. MRI-12665 shows a high speed straight line region, and a low speed straight line region joined at about 1800 RPM (slip equals one-half). Superposed upon these curves is the measured family of speed-torque curves, as a comparison: they agree quite will. In system design, one is usually interested in only a single region, the high speed region, or the low speed region. For most servo systems, which are of the position repeating type, interest lies in the low speed region since it is presumed that the system will almost always be near zero error point and hence the motor will be turning comparatively slowly. For velocity repeating servos, probably the high speed reguon is of greatest importance; but for such systems, both regions usually must be considered. It is interesting to observe, that for the FPE 25-11 motor, the slope of the low speed region is about 0.00028 ounce-inches per RPM, or a ratio of about three to one. These are typical servo motor characteristics.

We must consider assumptions (2) and (3). It can be seen from the family of speed-torque curves in Fig. MRI-12664 that assumption (2) is a good one. It is interesting that assumptions (2) and (3) are incompatable from purely geometric considerations; Fig. MRI-12666a, for instance has been constructed from a typical speed-torque curve for balanced operation by recourse only to assumption (2), that is, linear variation of torque at a specified speed. Such a construction yields a family of curves, all of which pass through a common point as shown, just as does the actual family of speed-torque curves. If the third assumption is applied to the diagram, that is linear variation of speed along a constant torque line, it will be noticed that it does not hold at all, especially near the synchronous speed point where all the curves bunch together. If one were to construct a family of curves using the balanced operation speed-torque curves and assumption (3), all the curves would again pass through a common point, but this time at the zero speed, maximum torque point; this, of course, is quite far from the actual case.

Summarizing, assumption (1) is usable provided interest lies in a low speed region or a high speed region. Assumption (2) is quite good and can be proved from the equations of the motor. Assumption (3) is not even geometrically compatable with the correct assumption, (2), and does not hold over large regions of the motor characteristic. A good case can be made for assumption (3), however, when considering only the low speed region, when certain idealizations are made.

D. Determination of the Parameters of the Two Phase Servo Motors

Part E of this section presents a method of determining the complete characteristics of two phase servo motors including input current (both amplitude and phase) as well as the complete family of speed torque curves. For such an analysis, a complete set of motor parameters is necessary. The measurement of the motor parameter (in the equivalent diagram) for these miniature, large air gap motors, must be performed differently than is usually done in ordinary polyphase motors. After the parameters have been determined for the typical servo motor used in this investigation, it will be apparent that the order of magnitude, of the parameters, for these special motors, is quite different from the relative magnitudes to be expected in the usual machine. The result is, that when using the conventional stall and no-load tests, it is necessary to interpret experimental data in a special way to get a consistent set of parameters.

The assumptions made by the author, referring to the equivalent circuit in Fig. MRI-12666b, are: (1) x_1 is approximately equal to x_2'; (2) r_m is approximately equal to zero; (3) the machine never saturates. It is not assumed and it would be wrong to do so, that under stall conditions, the magnetizing current is zero. Such an assumption leads to erroneous results, since the magnetizing current is high at all times due to the very large gap in servo motors. This situation is even more pronounced in the case of drag cup motors, since such a machine has two air gaps.

For usual machine construction, assumption (1) is a good one. This is because both rotor and stator, being mates, are similar geometrically. Even though they may look unalike, and their actual parameters differ markedly, when the rotor parameters are referred to the stator, the leakage reactances are approximately equal.

As the method of procedure is outlined, it will be seen that assumption (2) can checked for the motor being tested. Although only one motor has been checked by the author (and that one easily allows assumption (2)), it is to be presumed that servo motors, in general, due to their large air gap and low saturation, will all allow

assumption (2). Should assumption (2) not be allowable, an alternate procedure will be offered to take account of appreciable hysteresis and eddy current losses provided they are assumed to be constant over the range of operation.

Assumption (3) is accurate; tests reveal that even with double the rated voltage applied to the machine, the current drawn by the machine is almost perfectly sinusoidal. This is undoubtedly a consequence of the very large air gap which constitutes most of the magnetizing reactance.

If the aforementioned assumptions are made, only three easily performed tests need to be made to obtain the equivalent circuit of the machine.

(1) The machine is allowed to run at no load, with equal, balanced, and rated voltages applied to both phases. Under these conditions, the motor will run at almost synchronous speed, but this probably isn't necessary in most cases provided that no load speed is close to synchronous speed. When running in this manner, the input voltage and current are measured as well as the phase angle between them. The angle may be determined by oscillographic lissajous patterns or, if a suitable ranged wattmeter is available, it may be readily calculated from volt-ampere and watts data.

(2) The rotor is locked with rated voltage applied and the above measurements are repeated. If desired, the locked rotor torque can be measured, but such data is required only as a check on torque calculations.

(3) The stator resistance is measured with an ohmmeter with the motor disconnected from power sources.

Incidentally, all measurements should be taken with the motor at some constant temperature; it was found that "normal operation" could be construed to mean many things and that wide temperature variations can occur depending on the type of operation. The usual operating duty cycle of the machine should be determined in advance and such a cycle duplicated until the machine comes up to a stable operating temperature. For this investigation, it was assumed, as is the case for most servos, that the motor would be standing still for most of the time with full voltage applied to one phase, and no voltage applied to the other phase. (The zeroed case for a position repeating servo). Under this condition, the motor warmed up to about 90 or 100 degrees Fahrenheit, at which time r_1 equaled 260 ohms. All measurements were subsequently made with r_1 equal to 260 ohms; that is, a constant, but arbitrary temperature.

For the FPE 25-11, typical test data is as follows:

$$r_1 = 260\ \Omega$$

at no load: (speed is approximately 3520 RPM, slip = 80 RPM)

V_1 applied = 75V
I_1 = .069a
} angle between V app. and I = 74°

at locked Rotor:

V applied = 74V
I_1 = .092a
} angle between V app. and I = 34°

Torque = 2.2 ounce-inches

With the data from the no-load tests, and knowing r_1, the diagram in Fig. MRI-12666c may be constructed. This is the standard diagram for a machine running at, or near synchronous speed, that is, assuming no rotor current.

Fig. MRI-12666c shows thw impressed line voltage being balanced by a resistive drop, and a reactive drop in the motor. Referring to the equivalent circuit of the motor, and noting that the rotor (x_2' and r_2'/s) is assumed to be drawing no current, it is apparent that the resistive drop, V_r is given by:

$$V_r = I_1 (r_1 + r_m)$$

and the reactive drop V_x is given by:

$$V_x = I_1 (x_1 + x_m);$$

from which $(r_m + r_1)$ and $(x_1 + x_m)$ may be determined. It was found for this motor, as a typical servo motor, that

$$(r_1 + r_m) \doteq r_1,$$

as measured by an ohmmeter - for this machine, about 260 ohms. Therefore, $r_m \doteq 0$.

With the data from the locked rotor test, the parameters may be determined. If the rotor branch is assumed to draw current, it may be shown that

$$V_r = I_1 \left[r_1 + \frac{r_2' X_m^2}{(r_2')^2 + X^2} \right],$$

$$V_x = I_1 \left[x - \frac{X X_m^2}{(r_2')^2 + X^2} \right]$$

where

$$X = (X_2' + X_m) = (X_1 + X_m)$$

Since r_1 and the sum, $(X_1 + X_m) = (X_2' + X_m)$ are already known, one may readily solve for all the parameters. Note, that it is not necessary to ignore the magnetizing current in the stall test as others have done.[9]

The calculated parameters for the four watt FPE 25-11 are as follows:

$$r_1 = 260 \ \Omega$$
$$X_m = 980 \ \Omega$$
$$X_1 = X_2' = 50 \ \Omega$$
$$r_2' = 720 \ \Omega$$

The relative proportions of these parameters are far from what would be expected in the usual induction motor. It can be seen that x_1 and x_2' are quite small and could be neglected without too serious an error. From the data in test (1) it was determined that $r_m = 50$ ohms. While this is of the same order of magnitude as x_1 and x_2', and indeed, as much as one fifth of the stator resistance, it becomes negligible when placed in series with the quadrature impedance of 980 ohms presented by x_m. If, however, r_m had not turned out to be negligible in comparison with X_m, it would be possible to ignore the leakage reactances x_1 and x_2' and thereby have sufficient data from the two tests to calculate the parameters now assumed to be of significance. If it is desired to include x_1, x_2', and r_m, it will be necessary to make another measurement of input voltage, current and power at a third value of speed to obtain sufficient data to calculate all the parameters.

---

[9] See Koopman, op. cit.

This later type of calculation is likely to prove inordinately long and tedious compared to the ones previously outlined, and, except for unusual servo motors, will be unnecessary.

In order to check the results obtained with the data obtained from the no-load and stall tests, another measurement of input voltage, current, and power was made at a speed of 1800 RPM. Using the no-load data and the half-speed data, r_2' checked within 5% and x_2' within 25% of the values calculated with the no-load and stall data. The large variation in x_2' resulted because it is therefore difficult to separate from the data. Such a result shows the impracticability of trying to separate x_2' from x_1. The close agreement between the two values of r_2' is a far more significant result, and shows that the scheme outlined for the determination of the motor parameters is an accurate one.

E. Calculating the Static Performance of the Machine

Once the parameters of the motor have been determined, it is possible to compute both the magnitude and the phase of the input currents in both windings for arbitrary phase and amplitude of applied voltages. These calculations may be performed at any speed, and as a consequence, it is possible to predict the entire family of speed-torque curves. The method of performing these calculations will be based on the resolution of the two-phase motor into two single phase machines, coupled electrically by the rotating field of the motor and mechanically by the shaft of the motor. The equations presented will be perfectly general, allowing for: electrical unbalance of the applied voltages, as regards both phase and magnitude, external impedances in series with the machine, and inclusion of internal source impedances in the motor calculations. It is also possible to consider unbalanced machines. Needless to say, the simplest form of the equations result for the most perfectly balanced system. Usually it is only necessary to consider unbalance in the magnitude of the applied quadrature voltages.

The method of analysis of the two phase machine presented here has been developed by Dr. M.M. Liwschitz-Garil and presented in detail by Mr. Joseph Reed in a master's thesis at the Polytechnic Institute of Brooklyn (June, 1951), entitled "The Elimination of Centrifugal Switches in Single-Phase Induction Motors".

The circuit shown in Fig. MRI-12667a will be assumed to represent a single phase induction motor. It can also be considered to represent one phase of a two phase motor when that phase alone is carrying current. The correspondence between the parameters determined for the machine using the polyphase equivalent circuit and the single-phase diagram in Fig. MRI-12667a is one-to-one. That is, the results

of the determination of the parameters as outlined in section D, are used directly as indicated in Fig. MRI-12667a. $\dot{Z}_f$ is assumed to be the impedance across which is the voltage drop due to the forward rotating field of the motor; $\dot{Z}_b$ is the impedance presented by the backward rotating field. It may be readily shown that:

$$\dot{Z}_f = R_f + jX_f$$

$$R_f = 1/2 \cdot \frac{a(r_m + \frac{r_2'}{2S}) + b(k_2 X_m)}{(r_m + \frac{r_2'}{2S})^2 + (k_2 X_m)^2} \qquad (1)$$

$$X_f = 1/2 \cdot \frac{b(r_m + \frac{r_2'}{2S}) - a(k_2 X_m)}{(r_m + \frac{r_2'}{2S})^2 + (k_2 X_m)^2}, \qquad (2)$$

where

$$k_2 = 1 + \frac{X_2'}{X_m}$$

$$a = 1/4 \left[r_m \frac{r_2'}{S} - X_m X_2' \right]$$

$$b = 1/4 \left[r_m X_2' + \frac{r_2'}{S} X_m \right]$$

if $r_m \doteq 0$,

$$R_f = 1/2 \cdot \frac{\left(\frac{r_2'}{S}\right)}{\left(\frac{r_2'}{S} \cdot \frac{1}{X_m}\right)^2 + k_2^2}, \qquad (3)$$

and,

$$X_f = 1/2 \cdot \frac{\left(\frac{r_2'}{S}\right)^2 \frac{1}{X_m} + k_2 X_2'}{\left(\frac{r_2'}{S} \cdot \frac{1}{X_m}\right)^2 + k_2^2}. \qquad (4)$$

Also $\dot{Z}_b = jX_b$, where R_b and X_b are obtained from R_f and X_f by substituting (2-s) for s. The one phase of the motor may be represented as shown in Fig. MRI-12667b.

If we now consider the other phase of the two-phase motor and assume it to have (a) the number of effective turns as the first winding, but displaced 90 electrical degrees from the first winding, it may be represented as in Fig. MRI-12667c. In almost all servo motors, (a) is equal to unity.

If both windings are considered to be carrying current simultaneously, it can be demonstrated (see J. Reed, op. cit.) that:

$$\dot{V}_1 = \dot{I}_1 \dot{Z}_1 + \dot{I}_2 \dot{Z}_t, \tag{5}$$

$$\dot{V}_2 = \dot{I}_2 \dot{Z}_2 + \dot{I}_1 Z_q, \tag{6}$$

where

$$\dot{Z}_1 = (r_1+R_f+R_b) + j(X_1+X_f+X_b) + \dot{Z}_{s1} \tag{7}$$

$$\dot{Z}_2 = a^2(r_1+R_f+R_b) + ja^2(X_1+X_f+X_b)+a^2 Z_{s2} \tag{8}$$

$$\dot{Z}_q = a\left[(X_f-X_b) - j(R_f-R_b)\right] \tag{9}$$

$$\dot{Z}_t = a\left[(X_f-X_b) + j(R_f-R_b)\right]. \tag{10}$$

Z_{s1} and Z_{s2} are any impedances which may be placed in series with windings one or two, respectively. These may be, for instance, the internal impedances of the source driving the control winding or the impedance of the capacitor which is placed in series with the reference phase to provide quadrature voltage when the machine is operated from a single phase line.

Solving for the currents in the two phases:

$$\dot{I}_1 = \frac{\dot{V}_1 \dot{Z}_2 - \dot{V}_2 \dot{Z}_q}{\dot{Z}_1 \dot{Z}_2 - \dot{Z}_q \dot{Z}_t} = I_1 \angle \Phi_1 \tag{11}$$

$$\dot{I}_2 = \frac{\dot{V}_2 \dot{Z}_1 - \dot{V}_1 \dot{Z}_t}{\dot{Z}_1 \dot{Z}_2 - \dot{Z}_q \dot{Z}_t} = I_2 \angle \Phi_2 \tag{12}$$

The average torque is given by: (in ounce-inches)

$$T = \frac{135}{N_s}\left[(I_1^2 + I_2^2\, a^2)(R_f - R_b) + 2I_1 I_2 a(R_f + R_b)\sin\Phi\right] \quad (13)$$

Where Φ is the angle $(\Phi_2 - \Phi_1)$ and n_s is the synchronous speed of the machine.

When a = 1, the above equations reduce to the following:

$$\dot{Z}_q = (X_f - X_b) - j(R_f - R_b) \quad (14)$$

$$\dot{Z}_t = -(X_f - X_b) + j(R_f - R_b) = -\dot{Z}_q \quad (15)$$

$$T = \frac{135}{N_s}\left[(I_1^2 + I_2^2)(R_f - R_b) + 2I_1 I_2 \sin\Phi(R_f + R_b)\right] \quad (16)$$

The procedure for the complete calculation of the family of speed-torque curves may be outlined as follows:

(1) Given x_1, x_2^1, x_m, r_1, r_2^1, and assuming $r_m = 0$, calculate R_f, R_b, X_f, X_b at three or four different values of slip from zero to one, from equations (1) and (2) or (3) and (4).

(2) Using these, calculate $\dot{Z}_1$, $\dot{Z}_2$, $\dot{Z}_q$, $\dot{Z}_t$ from equations (7), (8) and either (9), (10) (14) or (15).

(3) At a specified slip, calculate the input currents for various voltages applied to the control phase of the motor according to equations (11) and (12).

(4) Calculate the torque at all the points for which the current has been determined in (3) according to equation (13) or (16).

Thus, points along lines parallel to the torque axis (constant speed, that is, fixed slip, s) corresponding to various applied control voltages have been calculated. Connecting the common voltage points, yields the familiar representation of the family of speed-torque curves. The complete calculation as outlined above is shown in Appendix IV.

It is now pertinent to discuss the validity of assumptions (2) and (3) as given in part C of this section in light of the theoretical development just presented. Considering assumption (2), the direct proportionality of torque to control voltage at a fixed slip, it is interesting to not that, for a fixed slip, the values of $\dot{Z}_1$, $\dot{Z}_2$, $\dot{Z}_q$, $\dot{Z}_t$, are fixed. If only one phase of the motor were connected to a source, the input

impedance would actually be a constant, independent of the applied voltage or the output torque, just as long as the slip remains constant. This has been varified very closely at a slip of one. (At this slip, the output torque is zero no matter what voltage is applied, because a single phase motor develops no torque.)

When both phases are excited a different situation prevails. The equations for the input circuit (11) and (12) show dependence on both applied voltages. Hence, it cannot be readily concluded that the input impedance is a constant, at a fixed slip, when V_1 and V_2 are both finite. It is to be noted that the quantities $\dot{Z}_g$ and $\dot{Z}_t$, the impedances which relate the dependence of the current in one phase upon the voltage applied to the other phase, are derived from the difference of R_f and R_b, X_f and X_b, while $\dot{Z}_1$ and $\dot{Z}_2$, the impedances which relate the dependence of the current in one phase to the voltage applied to the same phase are derived from the sum of these impedances plus the stator impedance. The difference quantities are always smaller than the sum quantities and markedly so for large values of slip (low speed region). When typical numbers are used, as in Appendix IV, the effect of the interaction of one winding on another is very small. The effect can be neglected except for the condition of full voltage on one phase and less than one third of full voltage on the other phase at slip near one-half. At slip greater than this, the effect on the current in one phase as a result of voltage on the other phase becomes less and less important, and disappearing completely at unity slip; at this point $R_f = R_b$ and $X_f = X_b$.

Having shown that the input impedance is approximately constant at a fixed slip, for wide variation of applied voltages, especially at large slip, we are now in a position to vindicate assumption (2). Reference to equation (16), giving the output torque as a function of the current in both phases, shows the torque to be composed of two terms. One of these, $(I_1^2 + I_2^2)$, is multiplied by $(R_f - R_b)$, a comparatively small term, especially at low speeds; the other term, $(2I_1 I_2 \sin\Phi)$, of the same order of magnitude as $(I_1^2 + I_2^2)$ is multiplied by $(R_f + R_b)$, a much larger number than $(R_f - R_b)$. Once again, Appendix IV, showing typical values of R_f, R_b as well as $(\Phi_2 - \Phi_1)$, lends numerical credance to these qualitative arguments. It can be seen that, assuming $(R_f - R_b)$ comparatively small and a fixed speed,

$$I_1 \sim V_1$$

$$I_2 \sim V_2 \ ;$$

the torque is, indeed, approximately proportional to the applied control voltage.

This is a very important conclusion for it shows that assumption (3) is essentially groundless from purely geometric considerations.

Fig. MRI-12664 shows that the actual family of speed-torque curves has the same general shape as the geometric construction in Fig. MRI-12666a except that the actual speed-torque curves do not pass through a common point. If the negative torque region of such a plot were extrapolated it would be seen that the various speed-torque curves tend to pass through a common point. The measured torque differs somewhat from the developed torque by windage and bearing losses, Fig. MRI-12668 shows the measured family of speef-torque curves extended back into the negative torque region. It shows how closely assumption (2) holds for a practical motor.

F. A Static Transfer Viewpoint of the Motor Extended to a Dynamic Viewpoint

One of the first considerations of a systems designer is the static accuracy requirement of the system. Such considerations based on the external mechanical load and static friction, lead to the initial estimates of the size of the system components. It is, therefore, pertinent to consider the static transfer characteristic of the two-phase motor. This may be readily extended to a dynamic consideration (provided electric transients within the motor are assumed to be fast compared to mechanical transients).

The input to the motor is a controlled AC voltage; the output is a torque at a speed. For a fixed input, both torque and speed may vary (usually the torque is considered to be the independent variable, but this is of no particular consequence). Such a device exhibits a three dimentioned manifold as an electrical description; as such, it is analogous to the vacuum tube.

It is to be noticed that although the input impedance of the motor (at the control input terminals) is not high, and does draw power, the magnitude of the input impedance is quite constant. We have seen that the angle of the input impedance is subject to considerable variation. If the device driving the two-phase motor has an output characteristic which is a function only of its input and the magnitude of its load impedance, and produces an output which is independent of the angle of the load impedance, the output of the driving device could be predicted on the basis of a fixed load which could have a fairly low impedance. One might extract the constant magnitude input impedance of the motor as an external element and regard the motor terminals exactly as one would regard the grid-cathode terminals of a vacuum tube.

Such a convenient viewpoint depends on the load voltage (i.e. the motor voltage) being independent of the power factor of the load on the motor driving device. If the motor driving device is a vacuum tube this is the case to a very good approximation. We will show later that it also happens to be the case for the push-pull circuit contrived from two doublers.

It is also to be noted that the three dimensioned manifolds describing both the motor and the vacuum tube are quite similar in general appearance. It is conceivable, therefore, that one might deduce an equivalent diagram of a motor similar to the one customarily used in linear vacuum tube circuit analysis. For example, consider the comparison chart shown in Fig. MRI-12669. In this chart we have shown quantities that may be considered analogous on opposite sides of the vertical line.

The manipulation of the three dimensioned vacuum tube characteristics is a well advanced practice. The chart shows how this technique is readily applicable to the two-phase motor. While the ensuing development can be made from nothing more than the geometry of the motor characteristics and without recourse to a different analogous device, nevertheless, the principle of analogy is a powerful one in aiding easy understanding.

The basis of the analogy which has been chosen, is the comparison of the plate characteristics of the vacuum tube with the speed-torque characteristics of the two-phase motor. Since these are two dimensioned plots of three dimensioned manifolds, there are two other equally descriptive families of curves for both devices. Any corresponding set would have been sufficient.

If one considers the low speed characteristics of the motor, say for slip greater than one-half (the usual case when the servo is in linear operation and not slewing), and draws them with an inverted abscissa as compared to the usual presentation, it is observed that the plate characteristics and the speed-torque curves are completely analogous, as regards their topological appearance, with the exception that the torque and e_b increase in opposite directions. One may then proceed to relate speed to i_b, torque to e_b, and applied control voltage to e_c. In linear vacuum tube theory, only two derivitive quantities are necessary to describe the AC performance of the vacuum tube. Three are generally considered, of which only two are independent. They are μ, the "amplification factor", defined as $\frac{\partial e_b}{\partial e_c}$ with the plate current held constant; r_p, the "plate resistance" defined as $\frac{\partial e_b}{\partial i_b}$ with e_c held constant; and g_m, the grid plate transconductance, or "mutual transconductance" - defined as $\frac{\partial i_b}{\partial e_c}$ with e_b held constant. It can be seen that the three derivitive quantities are related by,

$$\mu = g_m r_p$$

Since the vacuum tube is completely described by a three dimensioned manifold, only two of the three derivites are needed to specify performance completley when a static operating point (initial condition) is specified. For most circuit calculations the initial point is ignored since only AC variations about the initial point are of interest.

One can proceed immediately to define an analogous μ_m, r_{p_m}, g_{m_m} for the motor: μ_m is defined as $\frac{\partial T}{\partial V}$ with the speed held constant; r_{p_m} is defined as $\frac{\partial T}{\partial S}$ with the control voltage held constant; g_{m_m} is defined as $\frac{\partial S}{\partial V}$ with the torque held constant.

The vacuum tube may be represented by an equivalent circuit in terms of its derivitive quantities. The equivalent circuit of the motor has as its description the same three dimensioned manifold as that described the vacuum tube. The equivalent circuits are shown at the bottom of the chart, Fig. MRI-12669. The vacuum tube may be considered either as a voltage generator in series with a resistance (also r_p) and a set of external terminals to which any load may be connected. No matter what type of load is connected (in actual practice, the load must not be of such a nature so as to cause the tube to operate where it is three dimensioned manifold becomes very non-linear or fails to exist), it is but a simple matter to calculate both AC and DC performance to the tube about some static quiescent point. Similarly, for the two-phase motor, one may connect any external mechanical load in terms of its proper electrical analogue. In this regard, it is interesting to note that for the equivalent circuit deduced, electrical resistance and viscous friction are analogous quantities since:

$$r_{p_m} = \frac{\partial T}{\partial V} = \left[\frac{\text{OZ-IN}}{\text{RPM}}\right].$$

It is a simple matter to derive the electrical quantities analogous to the mechanical quantities inertia, and elastance. In the electrical circuit:

$$V = L \frac{di}{dt} .$$

We have compared torque with voltage, speed to current, therefore:

$$T = K \frac{ds}{dt}$$

where K is the quantity which, from the standpoint of the comparative differential equations of the two systems, must be analogous to L. In a mechanical system:

$$T = J \frac{ds}{dt}$$

where J is the moment of inertia and must be expressed in the proper units to correspond to those of μ_m, g_{m_m}, r_{p_m}. Therefore, by this simple comparison, electrical inductance is analogous to inertia. Similarly, elastance can be shown to be analogous to capacitance.

It is interesting to note that the quiescent point for the motor, in contrast to the vacuum tube, is zero torque output at zero speed with zero applied voltage. As a result, the values of speed and torque calculated by the equivalent circuit are those which actually obtain, whereas, to get the actual values for the vacuum tube, quiescent values have to be subtracted. In this regard, one notes that the motor is really equivalent to a push-pull amplifier and the speed-torque curves used in the analogy are actually only one half of a family that must extend symmetrically in opposite directions about the zero speed, zero torque point. This means only that the polarity of the equivalent speed or torque generator must reverse sign as the phase of the control voltage reverses.

IV Combination of Motor and Amplifier in Cascade

A. General Remarks

It is the purpose of this section to consider the effects of cascading motor and amplifier, particularly in regard to system calculations and system performance.

In Section II, we considered a magnetic amplifier suitable for the operation of two-phase servo motors in terms of performance with a passive, purely resistive load. It now becomes pertinent to consider such an amplifier with the type of load presented by a two-phase motor.

In Section III we presented the operating characteristics of the two-phase servo motor when operated by sinusoidal driving voltages in quadrature. However, the output of a magnetic amplifier is a peculiarly truncated sine wave containing odd harmonics of the same order of magnitude as the fundamental for certain regions of operation (near zero output).

From the standpoint of both performance and calculations, it would be desirable if the cascading of the motor and amplifier merely multiplies their respective transfer characteristics obtained by operating the amplifier with the usual resistive loads and driving the motor by sinusoidal voltages in quadrature. This is to say that the amplifier's operation is unchanged when an inductive, active load, is substituted for a resistive load and that the operation of the motor is the same for sinusoidal or non-sinusoidal excitation. Experimental evidence has been obtained which indicates that such conditions actually do obtain when certain reasonable stipulations are made.

A few words are in order regarding the complexity of operation of push-pull circuits. In the analysis of the simpler and more conventional magnetic amplifier circuits, there are one or two magnetic circuits to be considered, whereas there are usually four magnetic circuits in push-pull magnetic amplifiers. The simple circuits are usually idealized into one of two cases, the so called "free case" or the "restrained case"; these considerations greatly simplify the analysis. In current subtraction circuits, or voltage subtraction circuits with coupled loads, that have been contrivived from simple basic circuits, the simple members have as loads, active, reactive members consisting of circuits identical to themselves. That is each simple amplifier element has another amplifier element as part of its load; a load which is not only active, and reactive, but also non-linear.

We will describe in rather general terms, the effects of cascading the motor and amplifier in the case of the push-pull circuits and offer an explanation of why both motor and amplifier tend to operate in cascade as they did separately under ideal test conditions(i.e. resistive load for the amplifier and sinusoidal operation excitation for the motor).

B. Excitation of the Motor With Trucated Sine Waves

The output from the push-pull magnetic amplifier exciting the motor will, in general, be highly non-sinsoidal. The servo motor load is quite linear and does not saturate for rated applied voltages. The non-sinsoidal excitation may be considered to consist of a fundamental plus an array of harmonics; third, fifth, and so on.

It was desired to examine the motor performance with non-sinusoidal excitation, as derived from a magnetic amplifier, as compared with "pure" sine wave excitation. The pure sine wave, two-phase excitation was obtained by the use of the Scott-T connection from the three phase mains. The third harmonic content was measured to be about .1% with a harmonic analyzer; higher order harmonics were negligeble. Using this almost perfectly sinsoidal excitation (the angle between the two phases was as close

to ninety degrees as could be ascertained with a lissajous pattern) the set of speed-torque curves shown previously in Fig. MRI-12664 and as the dotted lines in Fig. MRI-12670 were obtained. Here, speed is plotted versus torque with the sine wave exciting voltage as a parameter.

Supperposed on the dotted curves, is a family of speed-torque curves (solid lines) obtained by using magnetic amplifier excitation. The parameter is the RMS amplitude of fundamental compenent (in this case 60 cycles) of the distorted exciting voltage. It is to be noted that these families of curves are almost identical, except near the zero speed, zero torque region. The obvious conclusion to be drawn from such results is that the motor responds only to the 60 cycle component of the exciting voltage appearing at its terminals - if the reference phase is excited with sinsoidal voltage.

As a further experimental check, an artifically derived excitation voltage was obtained by superposing upon a variable 60 cycle voltage a variable 180 cycle voltage. With the 60 cycle component set to zero, and with full voltage applied to the reference phase, no starting torque appeared as a result of the applied 180 cycle voltage, irrespective of phase relationship to the reference voltage up to an applied voltage of about 250 volts (maximum available). For any other magnitude of 60 cycle voltage, the motor delivered almost normal torque and speed no matter what magnitude of 180 cycle voltage was applied.

Since it is quite improbable that the third harmonic output will even become as large as the fundamental, under magnetic amplifier excitation, one may say with complete assurance, that only the 60 cycle (fundamental) component need be considered in predicting motor performance. Thus, the most significant transfer curve of the magnetic amplifier for servo motor work, is a plot of the fundamental component versus control current.

Several reasons for the insensitivity of the motor to the third harmonic of excitation voltage are as follows: to begin with, servo motors as a class are specifically designed not to develop torque under single phase operation at any speed. For a complete discussion if this, see Koopmen, (op. cit.). Part of this characteristic is due to the very high rotor resistance, which, while primarily designed to provide linear speed torque characteristics, also destroys any single phase characteristics the machine might have. It is well to note that with one phase open (and thus not acting as a damper winding) the machine develops almost zero stall torque, and a maximum torque of approximately .09 ounce-inches at 1800 RPM. This is a minute fraction of normal torque. Of course, the machine will not run at all if the second phase is shorted, so that if this phase is returned through a fairly low source impedance, the machine develops no torque due to single phase components in the excitation voltage.

It is well known also, that as a result of the very small physical size of these machines and the consequent limitations upon stator winding distribution, servo motors suffer a loss of torque as a result of a larger than normal, backward rotating field of third harmonic flux. This flux is created by space harmonics and is present even for perfectly sinusoidal excitation. It is quite possible that the loss of torque occasioned by applied single phase third harmonic voltage.

The clear cut experimental results, coupled with qualitative arguments are sufficient to enable one to say that only the fundamental component of the excitation voltage, no matter how distorted the excitation may be, need be considered in predicting motor performance.

It is pertinent to consider at this time phase variations between the fundamental component of the output of the magnetic amplifier and the magnetic amplifier supply voltage. Under the usual scheme of operation, two-phase voltage for the motor will be obtained from either a two phase line (generated as such, or derived from a three phase line) or from a single phase line with the reference phase of the machine supplied through a capacitor to provide, approximately, quadrature voltage.

In the case where there is a source of generated quadrature voltage (two phase line), one phase of the machine is connected to one phase of this line as reference and the other phase of the machine is driven from the second phase through the magnetic amplifier as a control device. In general, the fundamental component of the magnetic amplifier output will not be in phase with the sine wave voltage applied to the magnetic amplifier, and hence, not in quadrature with the voltage applied to the reference phase of the motor. This is a very significant fact, since the output of the two-phase machine is a function of the phase angle between the applied voltages as well as their amplitudes. Meserve and Steinhacker (see footnote No. 4) have shown that for a fixed speed, and fixed amplitude of applied voltages, the output torque is given approximately by:

$$T = K \sin\Phi$$

where Φ is the angle between the applied voltages and K is some proportionality constant depending on the various circumstances of operation. Stated another way, the torque that the machine would deliver for quadrature voltage excitation, is multiplied by the cosine of the angle between the voltage applied to the magnetic amplifier and the fundamental component of its output. Experimental results indicate that any phase shifts that may occur will probably by of no importance as regards system calculations, since proper adjustment of the magnetic amplifier as indicated in Section II will tend to minimize the phase shifts which do occur. If the phase shift should become large it would be necessary to take this into account in predicting system performance. Under such circumstances, the most pertinent transfer curve describing the magnetic amplifier

would be of the fundamental component of the output, multiplied by the cosine of the angle between it and the sine wave input to the magnetic amplifier, or the sine of the angle between it and the voltage of the reference phase of the motor, as a function of control current.

Such plots for push-pull current subtraction doublers, voltage subtraction doublers, or for that matter any type of amplifier producing output waveshapes of the type shown in Fig. MRI-12655, will not be significantly different from plots of only fundamental component versus control current for the reason that the phase does not change much until the zero output voltage point, whereupon it undergoes a 180 degree phase shift. This can be readily seen from the oscillographs in Fig. MRI-12671. If the bias is adjusted in the magnetic amplifier so that equal truncations are obtained on each side of the wave, the fundamental component of the output will always by in phase with the input and go through a 180 degree phase shift as the control current reverses. The only factor which may prevent operation in this manner is the possibility of excess circulating currents in the case of current subtraction circuits. (For voltage subtraction circuits, with completely split loads, there is no problem of this sort). In such case, it may not be possible to allow equal truncations and a certain phase shift of the fundamental component results. For the circuit used by the author, under resistive load, for greatest possible symmetry of truncation consistent with maximum allowable circulating current, the phase shift approached 45 degrees (cosine = .707) at 10% of the maximum output voltage. There is no reason to suppose that similar figures would not result for typical magnetic amplifier operation.

It will be recognized, that it is the phenomonon of truncation of both sides of the half sine waves that keeps the phase shift of the fundamental component low. For single ended stages with truncation on only side, and ignoring magnetizing current, the phase shift of the fundamental would approach ninety degrees, at zero output voltage. Figures MRI-12672 through MRI-12676a show the phase shift of the fundamental vs. control current for various values of bias and hence for various values of circulating current. Fig. MRI-12672 shows the characteristics for a doubler-type curcuit with a bias which allows a maximum circulating current of 500 milliamperes, (the maximum full-load current.) Here is shown the transfer curve of fundamental output voltage versus control current and the phase shift of the fundamental component with the quadrature voltage shown as reference. The phase of the fundamental of the output approaches to within 35 degrees of the phase of the quadrature voltage, hence it departs about 55 degrees from the phase of the supply voltage of the magnetic amplifier. That it does not shift 90 degrees is due to a small residual magnetizing current in phase with the

supply voltage which finally gets to be the same order of magnitude as the output - near the minimum output point. Fig. MRI-12673 shows the push-pull characteristic for the same amount of bias. Notice that the sine of the angle between the quadrature voltage and the 60 cycle output voltage doesn't depart appreciably from unity, until very low output voltages are reached.

Fig. MRI-12674 shows the push-pull characteristics for a reduced bias current allowing a maximum circulating current of one ampere (about twice that allowable for the cores used). It will be noticed, that due to the increased symmetry of truncation, the phase shift at the fundamental is less, for the corresponding output voltage than in the previous case. The same remarks apply to Fig. MRI-12675 except that here the bias was adjusted to provide almost perfect symmetry of truncation with the result that there is negligible phase shift through the amplifier. Such an adjustment allows a maximum circulating current of about three times that allowable, so that the amplifier could never be operated under such conditions.

For the case where the motor is operated from a single phase line and the reference phase is driven through a capacitor, all of the above remarks apply except that additional phase shifts may occur in the reference circuit as a result of impedance variations occurring as the motor operation varies. Such phase angle changes are always slight (See Appendix IV) and when the cosine is considered can be neglected.

C. Amplifier Operation With Active, Reactive Loads

All of the preceding remarks concerning phase shift of the fundamental component have been made regarding circuits producing doubly truncated waves when working into purely passive, resistive loads. Reference to Appendix IV shows that the motor is not at all a resistive load, and due to its back emf, is not a passive load. But it is interesting to note, that while the waveshapes at the output terminals of the magnetic amplifier are different for motor loading than for resistive loading, the transfer curves of fundamental output voltage versus control current are practically unchanged. The significance of such a phenomonen is that the amplifier performance may be determined on a basis of resistance loading and applied to motor loading. The author regrets that he is not able to justify these experimental results analytically and caution is urged in applying them, without verification to circuits other than current subtraction doublers.

Fig. MRI-12676a shows the type of wave shapes that are to be expected from a single doubler and a current subtraction coubler push-pull circuit under resistance load. Fig. MRI-12676b shows the voltage

across a highly inductive (but passive) load when only one of the doublers is connected it is significant that this wave shape is exactly the same as that produced by the inverse parallel thytatron circuit with inductive loading. (To obtain an inverse parallel thryatron circuit from a doubler, it is only necessary to replace each core and its associated rectifier by a thyratron). Notice that exactly the same situation occurs in the doubler with inductive loading, as does in the inverse parallel thyratron circuit with such a load. That is, the magnetic amplifiers "fires" at some point in the cycle, applying truncated voltage to the load. But because of the load's inductive character, the load current builds up from zero comparatively slowly, reaching a maximum near the end of the half cycle of supply voltage. Because the current may not cease abruptly in the inductive load, a negative integral of voltage across the magnetic amplifier core sufficient to unsaturate the amplifier is prevented until the current in the load diminishes to zero. Hence, the hang-on of current during the ensuing negative half cycle and the unusual fragment of the next half cycle applied to the load results. When the circuit is made into a push-pull amplifier by connecting another doubler, the operation is almost exactly the same, except that sometime in the half cycle after the first doubler saturates, the second doubler saturates and reduces the load voltage to zero. This hastens the extinction of the load current, but if the second firing is comparatively late in the cycle, the fragment of the next cycle that appeared across the load for a single doubler, can also appear for the push-pull doubler. This can be seen in the oscillographs in Fig. MRI-12676b.

Knowing now, at least qualitatively, the reason for the change of wave shape when resistive loads are replaced by inductive loads, we are in a position to offer a qualitative argument for the load voltage versus control current transfer curves being approximately the same for resistive as well as inductive loads. Considering the fundamental component of load voltage only, the inductive hang-on, while adding to this component during the beginning of each cycle, also prevents the normal firing until after the current diminishes to zero. In every case, such a hang-on delays the normal firing of the cycle. The tendency is to keep the fundamental component approximately constant. The phase of the fundamental componentof such a wave is more nearly in phase with the voltage applied to the magnetic amplifier than in the case of the normal waveshapes with resistive loads. This can be seen to result from the fact that the half cycles are more symmetrical about the 90 degrees and 270 degree points; thus inductive loads tend to bring the fundamental component of the output more nearly in phase with that applied supply voltage than do resistive loads.

Summarizing the case for inductive loads, we may say that the transfer curves of fundamental component of output voltage versus control current are approximately the same for inductive loads as resistive

loads and there is a tendency for the fundamental component to be more in phase with the supply voltage for the inductive case than for the resistive case. The inference from such a statement is obvious: the transfer curve of the magnetic amplifier is not appreciably affected by the power factor of the load.

We may now pass on to the active character of servo motor loads. This turns out to be a farily easy problem because the motor is only mildly active. Stated better, perhaps, its internal generator produces a small voltage in series with a large impedance. It is always 180 degrees out of phase with the voltage applied to the magnetic amplifier. During the time when the amplifier is not saturated, the impedance looking into it is quite high and a fairly large back emf may appear across the motor terminals. References to Appendix IV will show that this back emf is a maximum at synchronous speed and decreases to zero at zero speed. The characteristic of this generator voltage (i.e. voltage and impedance versus motor speed) is shown in Fig. MRI-12677. (This was obtained by driving the motor externally with only one phase connected to the line.)

When speed-torque curves are presented for a machine, it is implicitly assumed that this internal generator with its high internal impedance, is shortened out by the external source; that the voltage across the terminals is fixed externally. Of course, the impedance of the magnetic amplifier as a source of fundamental voltage is also quite low compared to the generator impedance associated with the back emf. Therefore, although during part of the cycle, a fairly large back emf may appear across the motor terminals, the fundamental component to which the motor responds is fixed by the magnetic amplifier.

The effect of the back emf is to change the effective voltage applied to the magnetic amplifier during the unsaturated time. The amount of this effect will depend upon the relative unsaturated impedance of the amplifier and the generator ompedance of the back emf. It is to be presumed, however, that at low speeds, the effect of the back emf will be quite small in producing significant variations in the transfer cirve of the magnetic amplifier.

V. A Summary of Significant Factors which Simplify the Design of Magnetic Amplifier Servo Systems

(1) The servo motor responds only to the fundamental component of the applied voltage multiplied by the sine of the phase angle between it and the reference voltage. For most cases, when the amplifier is biased so that the maximum circulating current is equal to the maximum load current, the sine of this angle is approximately equal to one over the useful range of magnetic amplifier output.

(2) the output voltage versus control current characteristics for the magnetic amplifier, contrived from current subtracting doublers, is approximately unchanged when resistive loads are replaced by inductive loads even though the output waveshapes may be quite different. The effect of the inductive load is to bring the sine term in (1) closer to unity.

(3) Since the motor input impedance is quite constant in magnitude and since its active character is, for the most part, negligeble, the magnetic amplifier transfer curves need only be obtained for the proper constant magnitude-impedance. Thus the voltage across the motor becomes a function only of the control current in the magnetic amplifier.

(4) The overall transfer characteristic of the motor and amplifier is thus given by the simple product of the amplifier transfer as obtained by sinusoidal excitation. (Amplifier transfer is two dimensioned because of the constant impedance load; the transfer of the motor is three dimensioned and can be treated by the equivalent circuit technique previously demonstrated). For instance, at a constant speed the motor transfer characteristic at locked rotor for sinusoidal qyadrature excitation is approximately .0028 ounce-inches per volt. In the linear range of the magnetic amplifier, its transfer characteristic for resistive load is approximately 10.2 volts per milliampere of controlled current. (Cores of set number 2, V_{ac} = 50 volts, bias = 35 milliamperes, maximum load current equals maximum allowable current equals 500 milliampers). The overall product is .0285 ounce-inches per milliampere. The actual overall characteristic of the amplifier dringing the motor is measured to be approximately .0255 ounce inches per milliampere.

(5) For mechanical transient conditions slow compared to electrical transients within the motor, the motor equivalent circuits may be readily applied to the dynamic case.

Appendix I

Description of the Magnetic Cores used in this Investigation

Two sets of four matched cores have been used in this investigation. Both sets have toroidally wound magnetic cores using Hipernik V, 0.002 in. tape. These cores were hand made by the Westinghouse Corporation and are matched to a tolerance not usually found in typical commercial equipment. This factor simplifies experimental results, because it eliminates certain extraneous discrepancies from test data. Set 1, the set of larger dimensioned cores, are capable of delivering in the push-pull connection, about 35 volt-amperes. The maximum motor load is about 7.5 volt-amperes. It is presumed that conservative design will result in internal source impedances considerably lower than the motor load impedance. In this regard, the results obtained with cores of set 1 are probably quite typical of that to be expected.

Tests were made with a smaller set of cores, set 2, which in the push-pull connection are capable of delivery only nine volt-amperes, or about the same as the maximum load. The results obtained using these cores (as regards comparative wave-shape across the motor, and inductive loads) are almost the same as the results obtained using the larger cores. This is to be expected since both cores provide an internal source impedance that is quite small compared to the motor impedance.

Set 1

Core Dimensions -	Outside Diameter	- 3"
	Inside "	- 2"
	Strip Width	- 2"
	Strip Thickness	- 0.002"
	Effective Area	- 0.8 square inches
Windings Used -	Control Windings	- 50 turns
	Load "	- 300 turns
	Bias "	- 40 turns

Set 2

Core Dimensions -	Inside Diameter	- 2"
	Outside "	- 21/2"
	Strip Width	- 1"
	Strip Thickness	- 0.002"
	Effective Area	- 0.4 square inches
Windings Used -	Control Windings	- 100 turns
	Load "	- 800 turns
	Bias "	- 40 turns

The motor used in this investigation has been discussed in detail in Sections III and IV. The physical dimensions are to be found in Fig. MRI-12661.

Appendix II

Oscillographic Method of Obtaining Magnetic Amplifier -TRANSFER CURVES

In order to simplify the obtaining of magnetic amplifier transfer curves an oscillographic technique was used that enabled the display of transfer curves on a long persistent oscillographic screen. Photographs of these displays constitute Figures MRI-12658a thru MRI-12658e. These are characteristics of current subtraction push-pull doublers. The displays show DC component of output voltage as a function of control current. They were obtained by rectifying and filtering the output of the magnetic amplifier to yield the DC output voltage, and by the use of a series of resistor in the control current circuit, also filtered, to yield a quantity proportioned to the control current. The control current was varied by a motor dirven potentiometer which required 28 seconds to cover the range of control current from +10 milliamperes to -10 milliamperes about zero current. As a result of this rather long time, there is no error introduced by the time constant of the amplifier response. In addition, the filters are sufficiently fast to clearly show hysteresis jumps.

The push-pull curves so obtained do not, however, cross the abscissa due to the manner of deriving the DC component of the output voltage, therefore a slightly different, but easily made interpretation, must be used by the observer. The push-pull curves obtained and presented in Figures MRI-12658a thru MRI-12658e are, for each bias setting a curve above the abscissa and one below. The curve above was obtained with control proceeding from left-to-right. This was done to bring out the possibility of double valuedness of the output voltage as a function of control current. This can occur, can be seen by Figures MRI-12658d and MRI-12658e, where the bias was sufficiently large to prevent overlap of the individual transfer curves. Such a phenomenon does not occur in Figures MRI-12658a, 12658b and 12658c where a more moderate bias was used.

Appendix III

Measurement of Speed-Torque Curves

The measurement of the speed-torque characteristics of servo motors is usually a somewhat difficult task. For instance, the machine used in this investigation, a typical servo motor, is capable of delivering a maximum power only four watts at its shaft (1/200 Horsepower). Maximum output torque of such machines is in the order of a few ounce-inches. If the machine is required to drive a tachometer, there is the possibility that a large fraction of the very meager output torque may be used in driving the tachometer, particularly at higher speeds. Alternately stroboscopic measurements may be used, but these are tedious, lengthly and complicated by the difficulties of detecting rotating speed by the apparent cessation of motion as well as related problems of multiple and sub-multiple synchronization.

At the beginning of this investigation, it was anticipated that numerous speed measurements would be required; to facilitate these measurements, a device was constructed which measures the speed of a rotating shaft, yielding the speed continuously in the manner of a tachometer, yet presenting negligible load even to a 1/200 Horsepower motor. The operation of this non-loading tachometer is as follows:

A three inch diamerer aluminum disk weighting about 1/4 of an ounce is attached to the motor shaft. This shaft has a series of small holes near its periphery, and is interposed between a lamp and a photocell. As the shaft rotates, the lamp shining through the holes, produces periodic bursts of illumination on the photocell. The frequency of these bursts is a direct measure of the speed of rotation.

The bursts of light are converted by the photocell into electric pulses, which after suitable shaping and limiting, are used to trigger a thyratron in parallel with a charginh condenser. A d'Arsonval meter is placed in the plate circuit of the thyratron. The calibration of the instrument is a fairly straight line on a logarithmic plot except for very low speeds.

The tachometer may also be used to determine dynamic accelerations. If a probe is placed at the grid of the thyration to intercept the triggering pulses, the change of spacing between pulses displayed on a linear time base, gives instantaneous acceleration. A quantitative measurement can be made as follows:

The phenomenon initiating the acceleration may be used to trigger a slow driven sweep of an oscilloscope (Dumont type 304, for instance). If the resulting sweep is photographed, or displayed on a long persistance screen, a quantitative calculation may be easily performed if the speed of the sweep is known. If this is not known, a suitable marker may be added to the sweep, or a second sweep may be used.

Torque

Torque measurement can also present some problems. The technique used in this investigation is as follows:

The torque was measured at a 1/4 inch diameter shaft which was made as a part of the holed speed measuring disk. The maximum torque of the machine was (at stall) about two ounce-inches for 65 volts applied to each phase. This meant an actual pull on the string of about eight ounces, or a half pound.

Usual prony brake procedure dictates the use of two scales with net torque being given by the difference in the readings, since the brake band tension does not constitute torque output. To simplify measurements, and because the measurement could be accomplished with ordinary sewing - machine thread on the loading shaft, the need for the second scale was obviated by merely wrapping the thread around the shaft several times with the free end of the thread left free. Since the tension in the string where it leaves the shaft for the scale is proportioned to the e^{th} (e=2.118) power of the angle of wrap times the tension in the free end of the string, only a few turns are necessary to load the motor. As a result, the difference between the tension at the start of the wrap and the finish of the wrap was almost identical to the scale reading, consequently only one reading was necessary and it was possible to obtain finger tip control of the speed.

Appendix IV

The Calculation of the Complete Family of Speed-Torque Curves For a Typical Servo Motor (Diehl FPE 25-11)

Referring to Section IV, the FPE 25-11, as a typical servo motor, has (a) the turns ratio between the windings equal to unity. Therefore, the simplied equations (3), (4), (14), (15), for $\dot{Z}_f$, $\dot{Z}_b$, $\dot{Z}_o$ and $\dot{Z}_t$, and (16) for torque apply. The parameters of the machine, as found according to the methods of chapter IV are as follows (assuming the usual equivalent diagram for the balanced machine as shown in Fig. MRI-12666b):

$$r_1 = 260\ \Omega$$
$$x_1 = x_2' = 50\ \Omega$$
$$x_m = 980\ \Omega$$
$$r_m = 0$$
$$r_2' = 720\ \Omega$$

The procedure is as follows:

(1) Calculate R_f, R_b, X_f, X_b for slip equal to 1, 3/4, 1/2, 1/4 according to equations (3), (4), (14) and (15).

(2) Using these values, in equations (11), (12) calculate $\dot{I}_1$ and $\dot{I}_2$ for fixed voltage $\dot{V}_1$ of 65 volts and a variable voltage $\dot{V}_2$ varied in the steps 5, 15, 25, 35, 45, 55 and 65 volts, at several values of fixed slip.

(3) Using these values of current, calculate the corresponding values of torque.

(4) Plot the results.

(1) Calculating R_f, R_b, X_f and X_b.

Sample calculation: let $s = 1/2$.

$$R_f = \frac{1}{2} \quad \frac{\frac{r_2'}{s}}{\left(\frac{r_2'}{s}\frac{1}{xm}\right)^2 + k_2^2}$$

$$X_f = \frac{1}{2}\,\frac{\left(\frac{r_2'}{s}\right)^2 \frac{1}{x_m} + k_2 x_2'}{\left(\frac{r_2'}{s}\,\frac{1}{x_m}\right)^2 + k_2^2}$$

$$k_2 = 1 + \frac{x_2'}{x_m} = 1\,\frac{50}{980} = 1.051$$

$$R_f = \frac{1}{2}\,\frac{1440}{\left(\frac{1440}{980}\right)^2 + 1.051^2} = 221.\ \text{ohms}$$

$$X_f = \frac{1}{2}\,\frac{\frac{(1440)^2}{980} + 1.051(50)}{3.262} = 332.\ \text{ohms}$$

$$R_b = \frac{1}{2}\,\frac{480}{\left(\frac{480}{980}\right)^2 + 1.051^2} = 179.\ \text{ohms}$$

$$X_b = \frac{1}{2}\,\frac{\frac{480}{980}^2 + 1.051(50)}{1.342} = 108.\ \text{ohms}$$

from which $\dot{z}_1$, $\dot{z}_2$, $\dot{z}_t$ and $\dot{z}_q$ can be found.

$$\dot{z}_1 = (r_1 + R_f + R_b) + j(X_1 + X_f + X_b) = \dot{z}_2 = 660 + j490$$

$$\dot{z}_q = (X_f - X_b) - j(R_f - R_b) = 224 - j42 = \dot{z}_t$$

(2) Calculation of motor currents:

$$\dot{I}_1 = \frac{\dot{V}_1\dot{z}_2 - j\dot{V}_2\dot{z}_q}{\dot{z}_1\dot{z}_2 - \dot{z}_q\dot{z}_t}$$

$$\dot{I}_2 = \frac{j\dot{V}_2\dot{z}_1 - \dot{V}_1\dot{z}_t}{\dot{z}_1\dot{z}_2 - \dot{z}_q\dot{z}_t}$$

for $V_1 = V_2 = 65$ volts.

$$I_1 = \frac{65(660+j490) - j65(224-j42)}{(660+j490)^2 + (224-j42)^2}$$

$$I_1 = 0.064 \angle -45.2^\circ \text{ amps.}$$

$$I_2 = jI_1 = 0.064 \angle +44.8^\circ \text{ amps.}$$

The actual measured results yield (See Section IV) $I_1 = 0.066 \angle -46.0^\circ$. This high degree of correlation follows in all the current calculations. Fig. MRI-12678 shows the plot of I_1 and I_2, predicted and measured for slip = 1/2, as a function of V_2.

After carrying through similar calculations for $V_1 = 65$ volts and $V_2 = 45, 35, 25, 15, 5$ volts, the results may be tabulated as follows:

V_2	V_1	I_2	I_1
65	65	$0.064 \angle 44.8$	$0.064 \angle -45.2$
55	65	$0.053 \angle 42.8$	$0.066 \angle -42.8$
45	65	$0.041 \angle 36.8$	$0.068 \angle -41.3$
35	65	$0.030 \angle 27.8$	$0.071 \angle -41.1$
25	65	$0.021 \angle 11.2$	$0.073 \angle -37.1$
15	65	$0.015 \angle -22.9$	$0.075 \angle -35.1$
5	65	$0.018 \angle -65.8$	$0.077 \angle -31.3$

The plot of this data, compared to the measured data is shown in Fig. MRI-12678.

It is to be observed that I_1, changes only slightly whereas I_2 changes markedly, particularly as regards its angle. Where the angle of I_2 lags behind V_2 more than 90°, (where the magnitude of the angle of I_2 is negative in the above table), that winding becomes a generator and part of the power put in the reference winding is delivered at its terminals. If V_2 is decreased still further, the machine develops no output torque and, of course, will not run at slip = 1/2. To be sure, under these conditions the machine becomes a brake.

(3) Calculation of Torque

Using the values of I_1 and I_2 for the various voltages, V_2 at this fixed slip of 1/2, using equation 13, it is now possible to compute the torque.

$$T = \frac{135}{n_s}\left[(I_1^2+I_2^2)\ (R_f-R_b) + 2I_1I_2\sin\Phi(R_f+R_b)\right]$$

A word of caution is on order regarding the sine term. It will be recalled that Φ was defined as $(\Phi_2-\Phi_1)$, where Φ_2 is the phase angle between V_1 and I_1. For the tabulated currents, it will be noticed that the sign of the sine term is positive except for very low values of V_2. This is physically correct; the two torque terms must add for balanced voltage, they subtract only for large unbalances when the argument of the sine term becomes a negative angle. It is to be noted that had the voltage V_1 been assumed to lead V_2 instead of lag it, the sign of the sine term would have been negative; this, of course, is not correct, and will not yield the proper family of speed-torque curves, although the only physical difference, as regards the motor operation, between the two cases, would be a reversal in direction of rotation.

For V_1V_2 = 65 volts.

$$T = \frac{135}{3600}\left[(0.064^2+0.064^2)(221-179)+2(.064)(.064)\sin 90^\circ(221-179)\right]$$

$$T = 1.36 \text{ oz.-in.}$$

V_2	65	55	45	35	25	15	5
T	1.36	1.13	0.922	0.680	0.443	0.162	-0.123

If these calculations are performed at S = 1/4, 3/4 and 1, the following tables of motor operation may be prepared.
For slip = 1 and V_1 = 65 volts.

V_2	T	I_1 (MA)	I_2 (MA)
65	2.18	83.8 /-28.7	83.8 /61.3
55	1.86	↓	70.9 /61.3
45	1.52		58.0 /61.3
35	1.18		45.2 /61.3
25	.843		32.2 /61.3
15	.506		19.3 /61.3
5	.169		6.45 /61.3

For slip = 3/4 and V_1 = 65 volts.

V_2	T	I_1	I_2
65	1.84	0.0725 /-37.5	0.0725 /52.5
55	1.56	0.0736 /-36.6	0.0602 /57.4
45	1.27	0.0752 /-35.8	0.0477 /49.5
35	0.968	0.0764 /-34.8	0.0354 /40.8
25	0.657	0.0778 /-34.6	0.0234 /40.7
15	0.345	0.0795 /-33.3	0.0118 /22.5
5	0.120	0.0795 /-33.3	0.0134 /-30.8

For slip = 1/4 and V_1 = 65 volts.

V_2	T	I_1	I_2
65	.825	.0612 /-59.1	.0612 /30.9
55	.690	.0628 /-54.9	.0500 /25.6
45	.529	.0652 /-51.1	.0398 /17.8
35	.369	.0678 /-47.1	.0250 /10.2
25	.168	.0705 /-44.2	.0245 /-16.4
15	-.057	.0732 /-41.1	.0231 /-45.3
5	-	.0764 /-36.6	.0276 /-70.9

S	R_f	R_b	X_f	X_b	$\dot{Z}_1$	$\dot{Z}_g$
1	210	210	161	161	680+j372	0
.75	233	191	241	135	690+j426	106-j42
.5	221	171	332	108	660+j490	224-j42
.25	147	161	437	38.5	568+j576	326-j14

It will be noted that at speeds for slip = 1/2 or greater, the calculated values are about 20% high. If a torque measurement can be made as outlined in the section on the determination of parameters, the entire family can be multiplied by a correcting factor and so be made to yield even closer results. Since only one correcting factor is needed, only one torque measurement need be performed.

BIBLIOGRAPHY

1. Chesnut and Mayer, Servomechanisms and Regulating Systems Design. Vol. I, New York, John Wiley & Sons, Inc. 1951.

2. Cohen, Sidney B., Analysis and Design of Self-Saturable Magnetic Amplifiers. I.R.E. Proceedings, Sept. 1951.

3. Geyger, W.A.. Magnetic Amplifiers of the Balance Detector Type - Their Basic Principle, Characteristics and Applications. AIEE Proceedings, Vol. 70, 1951.

4. Koopman, R.J.W., Operating Characteristics of Two Phase Servo Motors. AIEE TRANSACTION, Vol. 68, New York, 1949.

5. Liwschitz-Garik and Whipple, Electrical Machinery, Vol. II, New York, D. VonNostrand Co. Inc., 1946.

6. Meserve and Steinhocker, Two Phase A-C Servo Motor Operation For Varying Phase Angle of the Control Winding Applied Voltage. AIEE, Technical Paper 51-366, August 1951.

7. Reed, Joseph, The Elimination of Centrifugal Switches in Two Phase Servo Motors. Thesis, Polytechnic Institute of Brooklyn, June 1951.

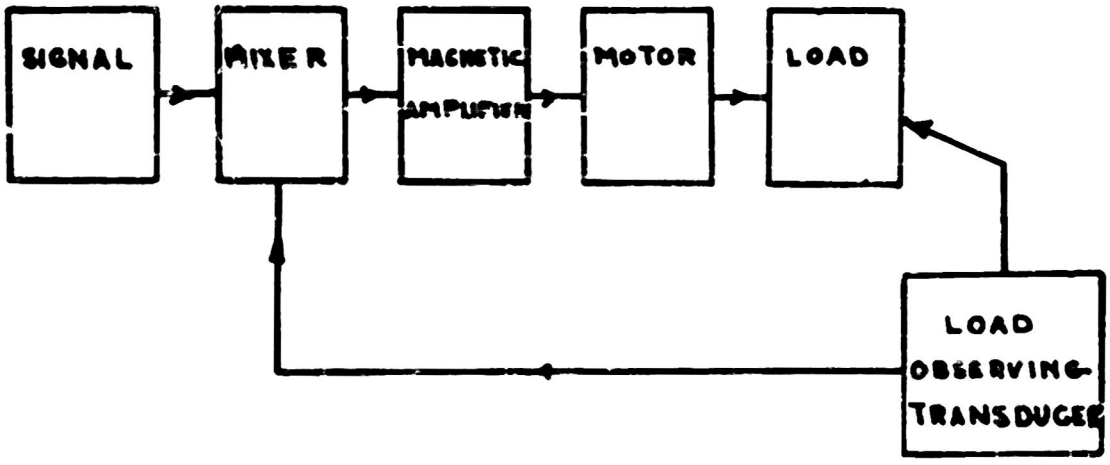

BASIC MAGNETIC AMPLIFIER, ELECTRIC MOTOR SERVO

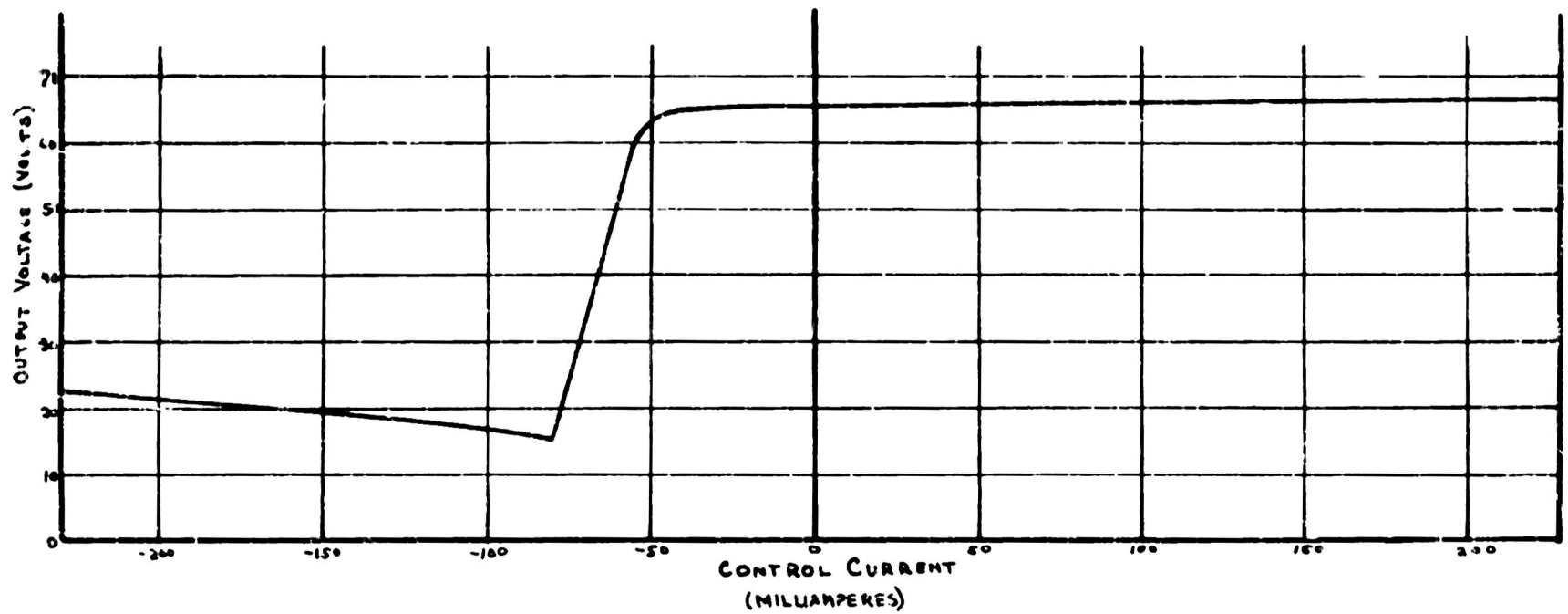

TYPICAL TRANSFER CURVE FOR A SENSITIVE MATERIAL MAGNETIC AMPLIFIER

(SET #1 CORES ; DOUBLER CONNECTION; NO BIAS MMF)

TYPICAL SELF SATURATING MAGNETIC AMPLIFIERS

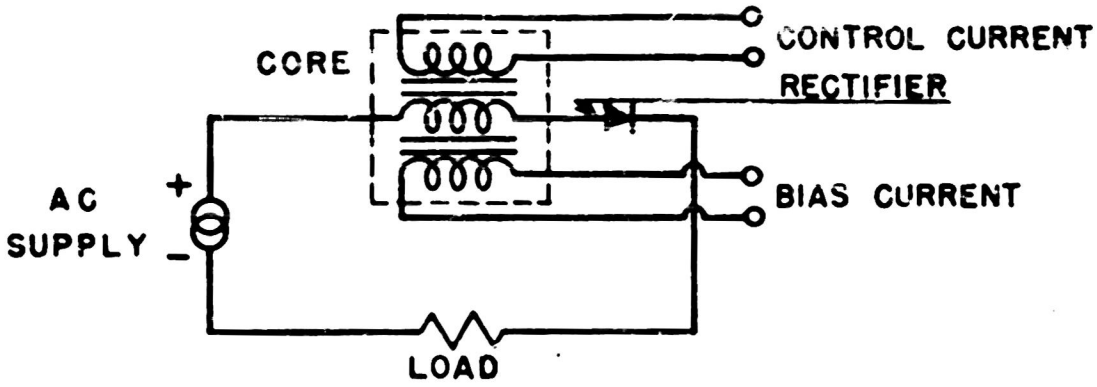

"HALF WAVE" CIRCUIT

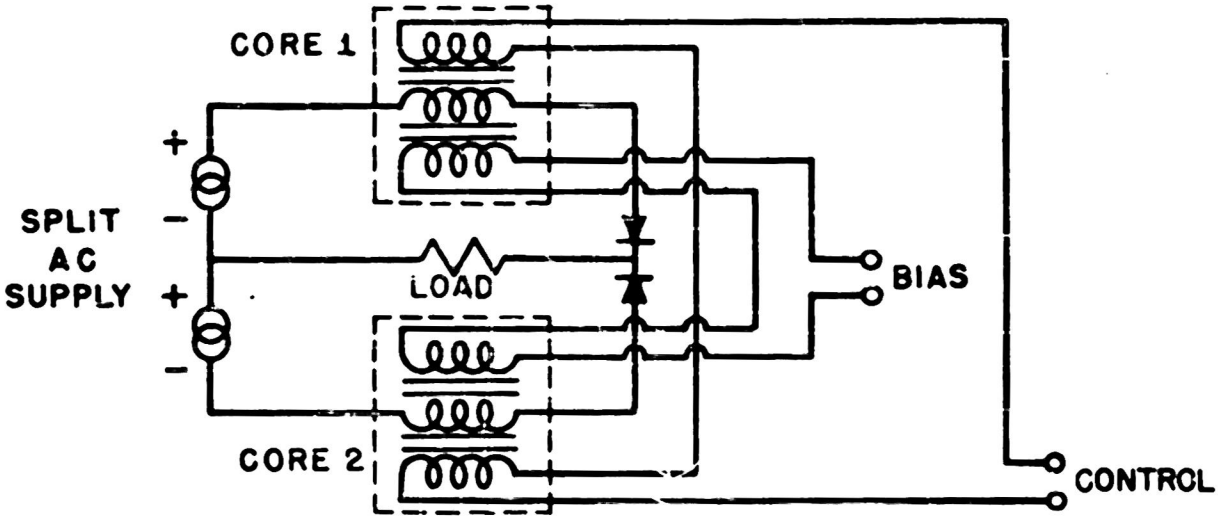

"FULL WAVE" CIRCUIT

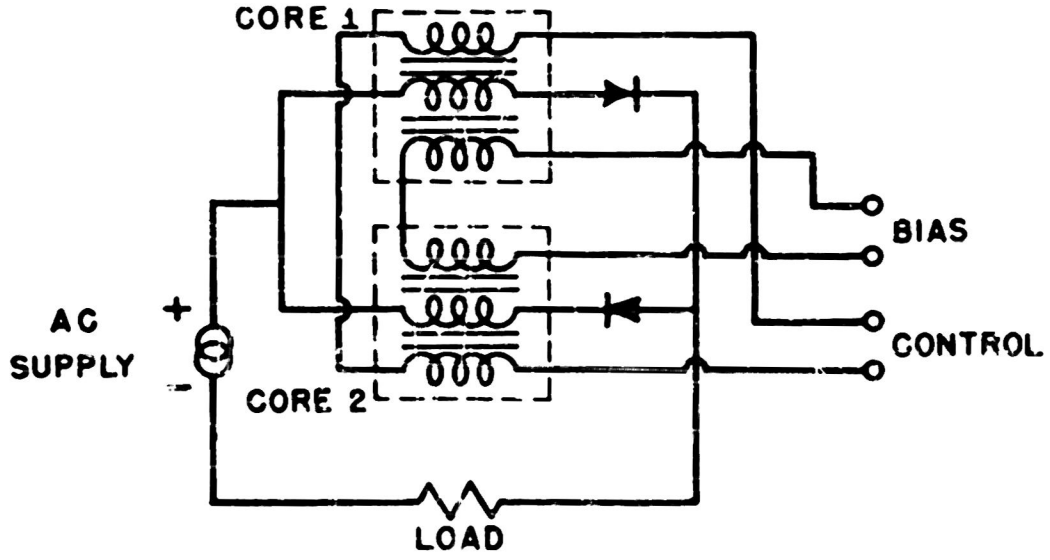

"DOUBLER" CIRCUIT

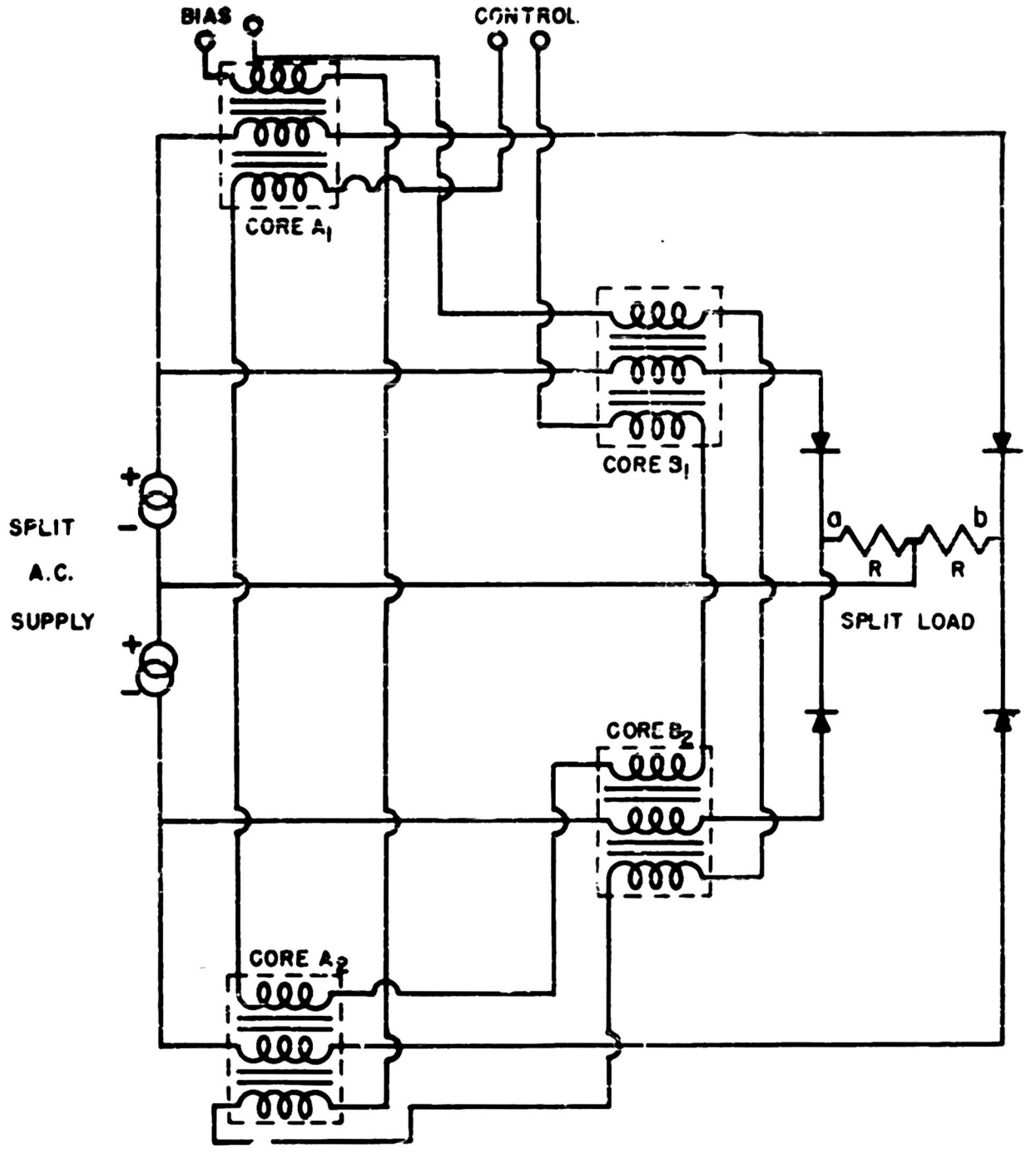

PUSH-PULL CIRCUIT COMPOSED OF TWO FULL WAVE CIRCUITS

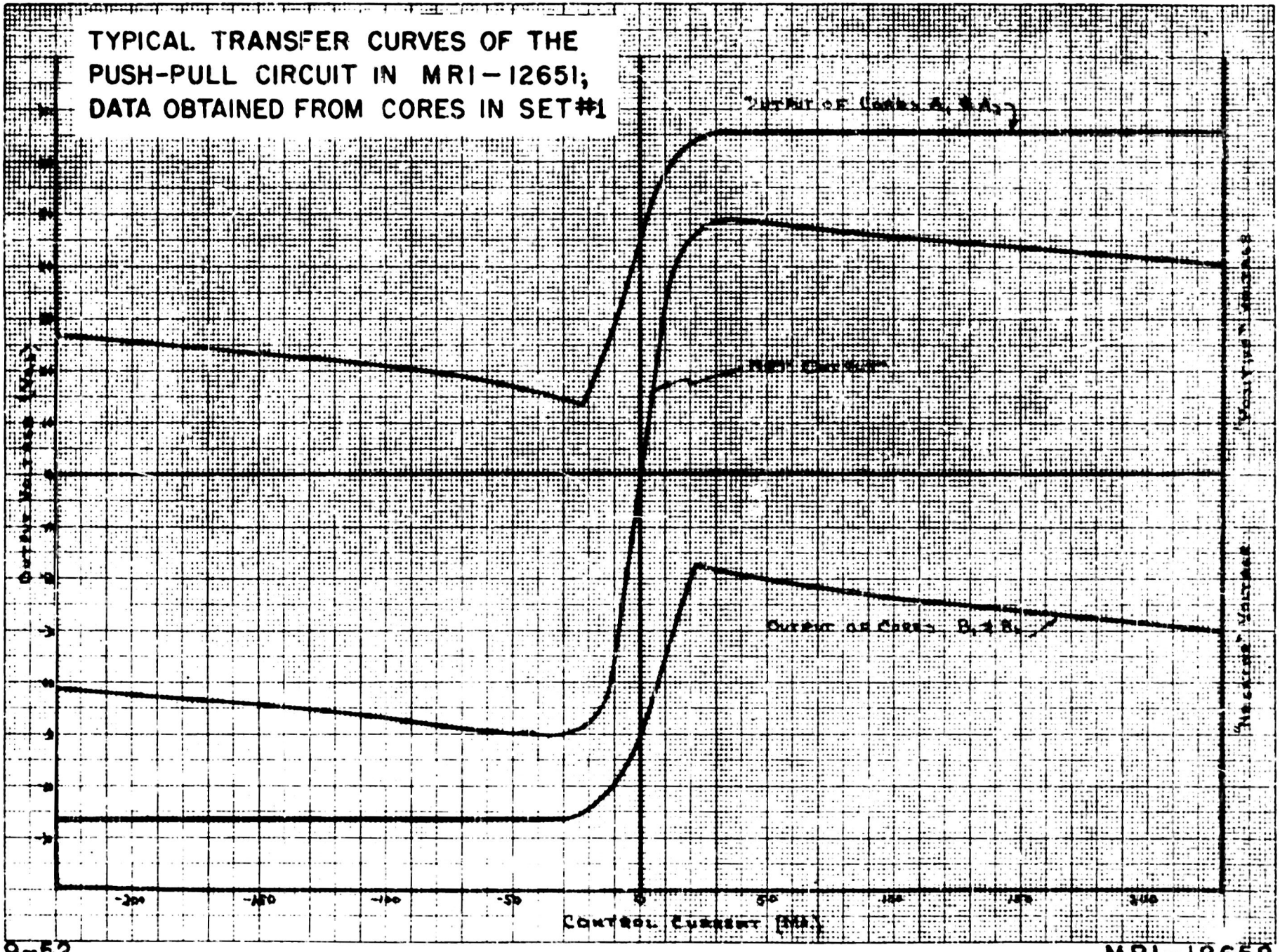
TYPICAL TRANSFER CURVES OF THE
PUSH-PULL CIRCUIT IN MRI-12651;
DATA OBTAINED FROM CORES IN SET #1
Output of Cores A1 & A2
Output of Cores B1 & B2
Control Current (ma.)

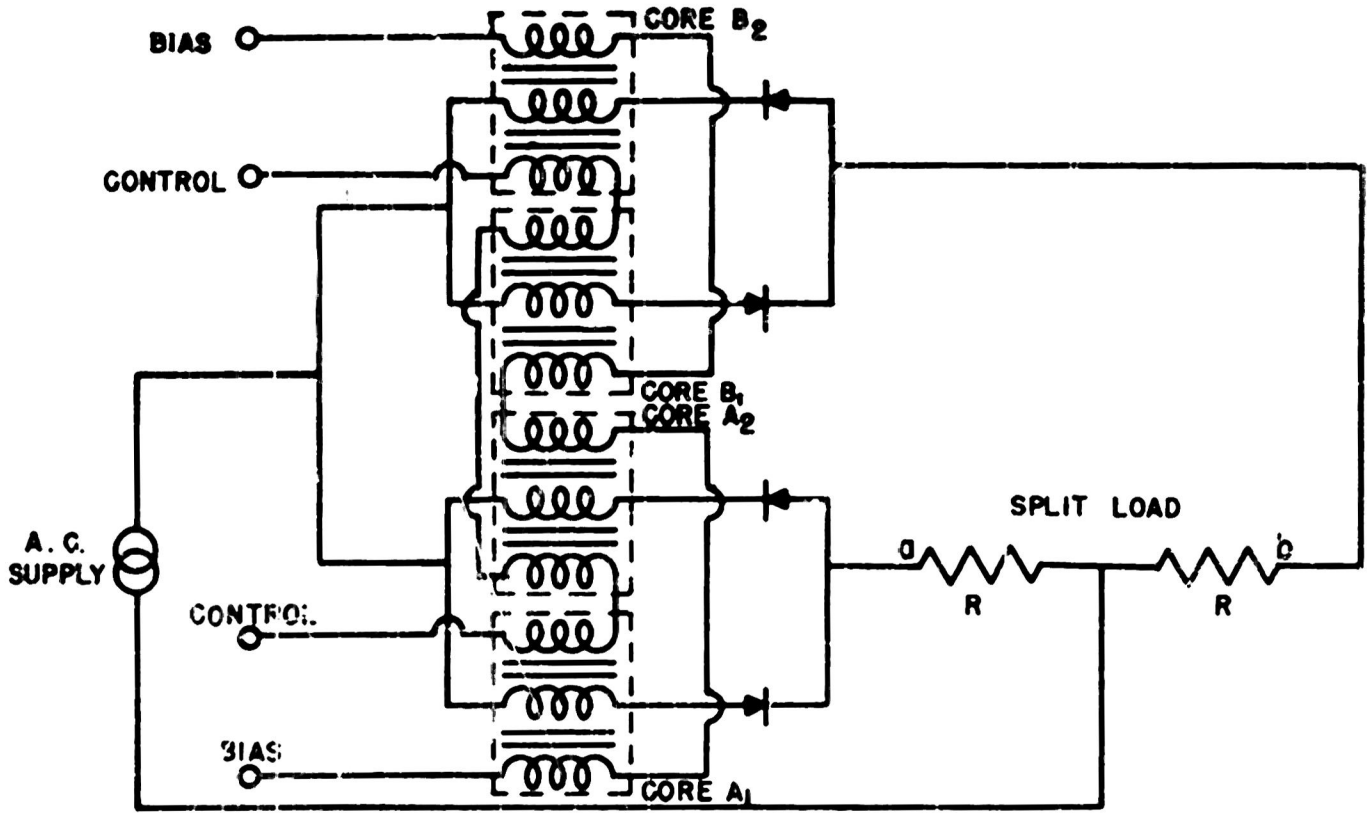

PUSH-PULL CIRCUIT COMPOSED OF TWO DOUBLERS

MRI-12653

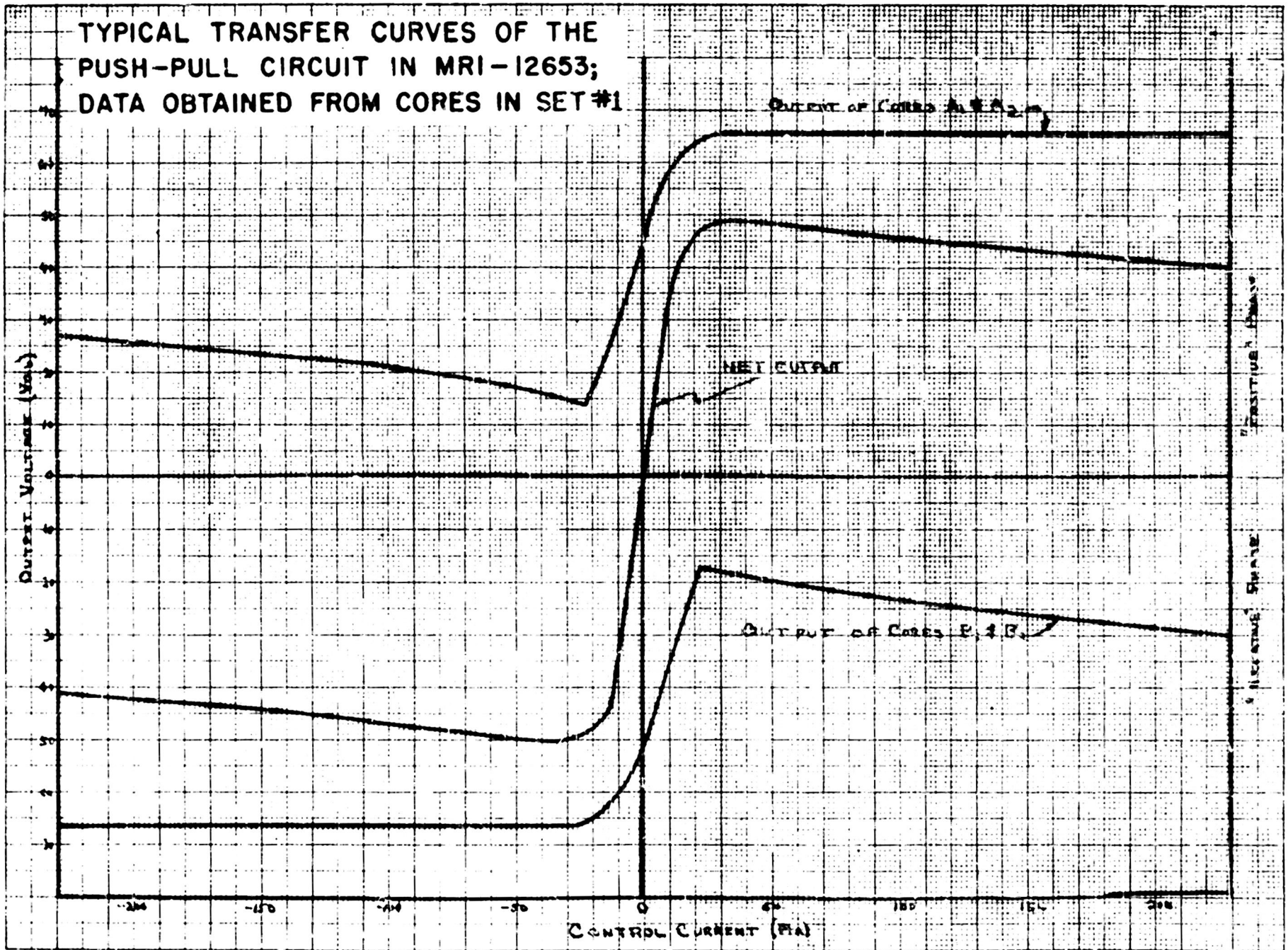

9-52

MRI-12654

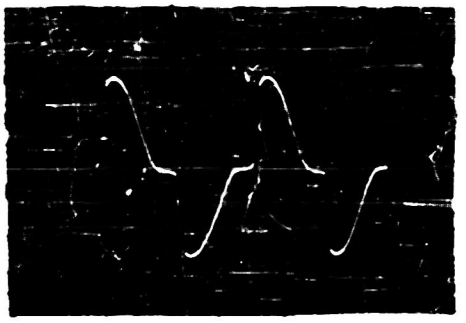

Typical Output of the Doubler Composed of Cores A_1 and A_2

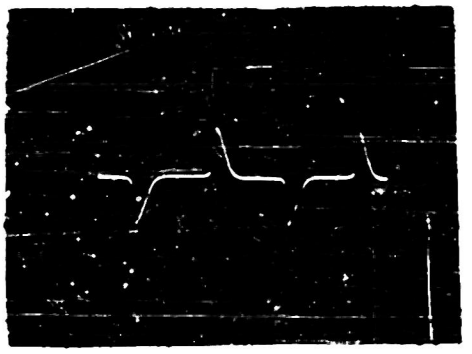

Corresponding Output of the Doubler Composed of Cores B_1 and B_2

Net Subtracted Output of the Two Doublers Across the Split Load

Doubly Truncated Output of the Push-Pull
Doubler Circuit shown in MRI-12[illegible]4

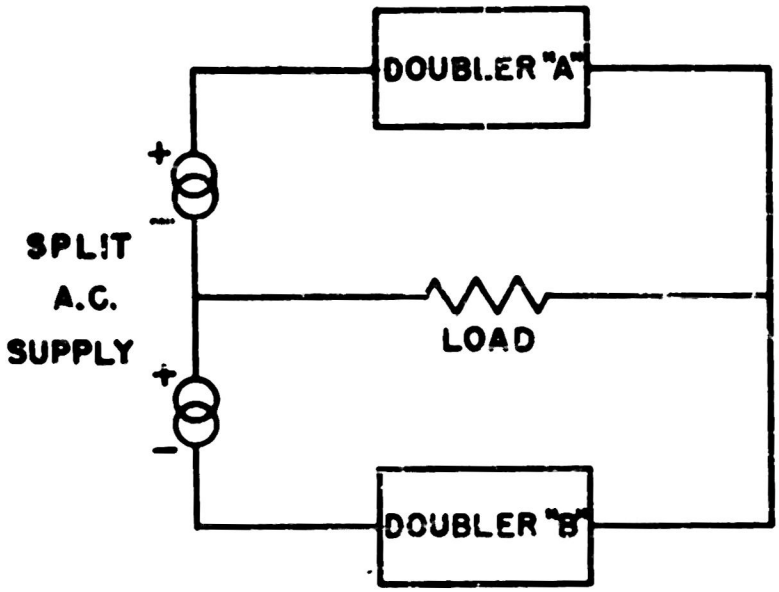

PUSH-PULL CURRENT SUBTRACTION DOUBLER

(a)

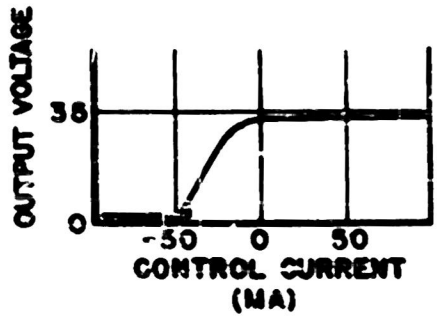

TRANSFER CURVE OF ONE DOUBLE FROM THE CORES OF SET #1 WITH NO BIAS

(b)

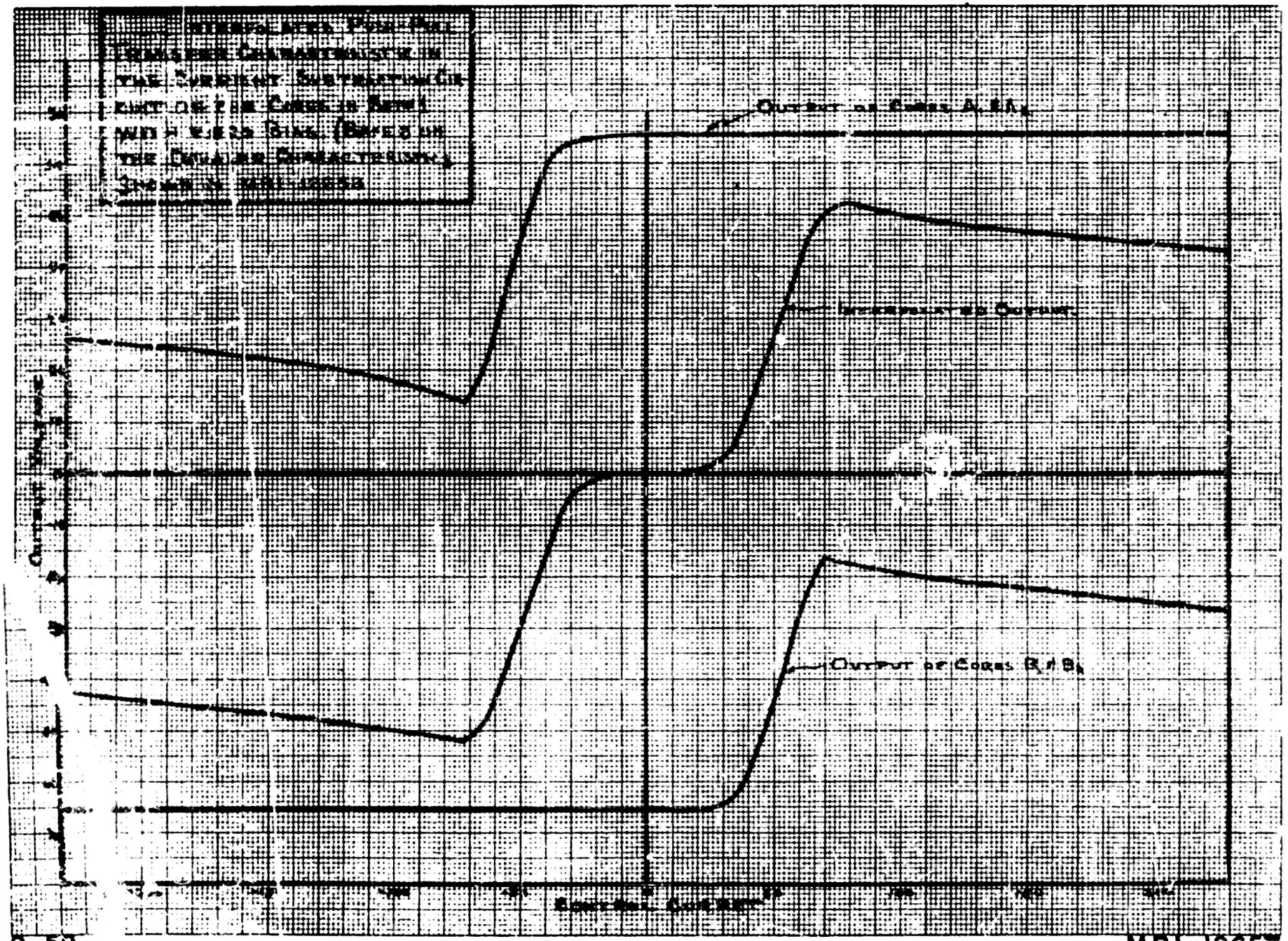

9-52

MRI-12657

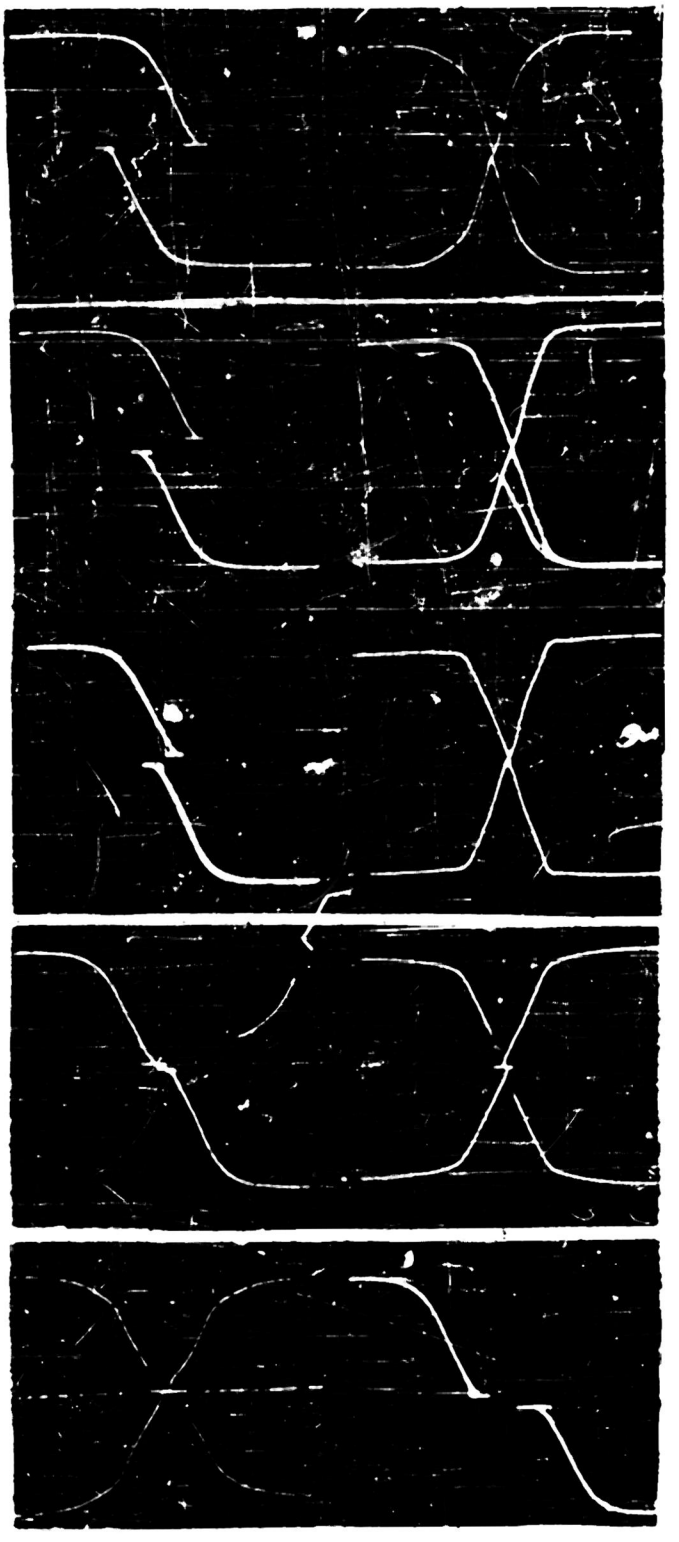

(a)
Bias = 250 milliampere-turns

(b)
Bias = 280 milliampere-turns

(c)
Bias = 320 milliampere-turns

(d)
Bias = 360 milliampere-turns

(e) = 400 milliampere-turns

Oscillographic transfer curves of the push-pull current subtraction doubler circuit showing the relative position of the individual doubler transfer characteristics before making the push-pull connection, as well as the actual push-pull transfer characteristics. Curves obtained with the cores of set No. 1; total AC supply = 70 volts; maximum load voltage = 25 volts; maximum load current = 440 milliamperes. The ordinates are at 50 milliamperes control current (250 milliampere-turns). Bias for each set of curves, as noted above.

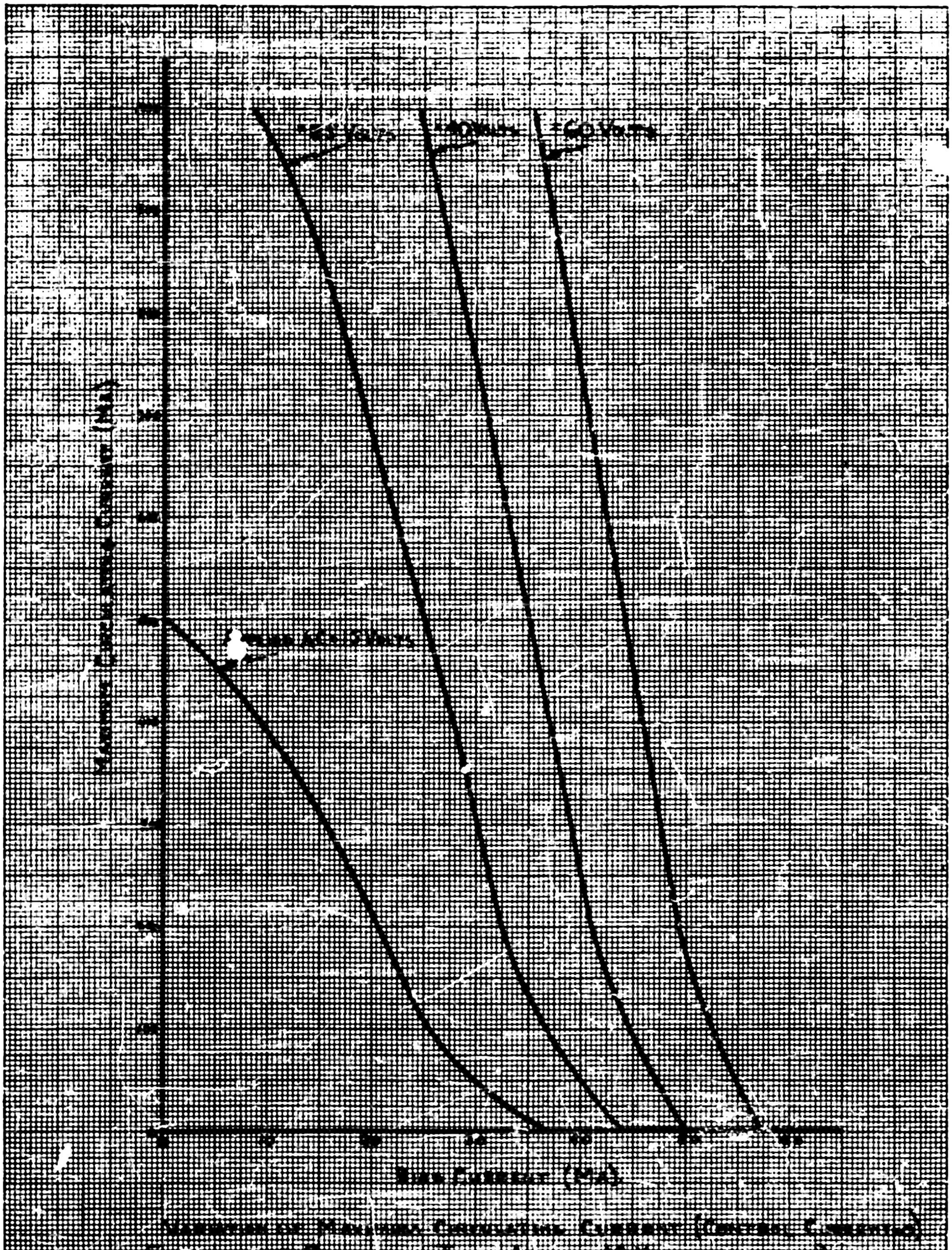

[illegible]

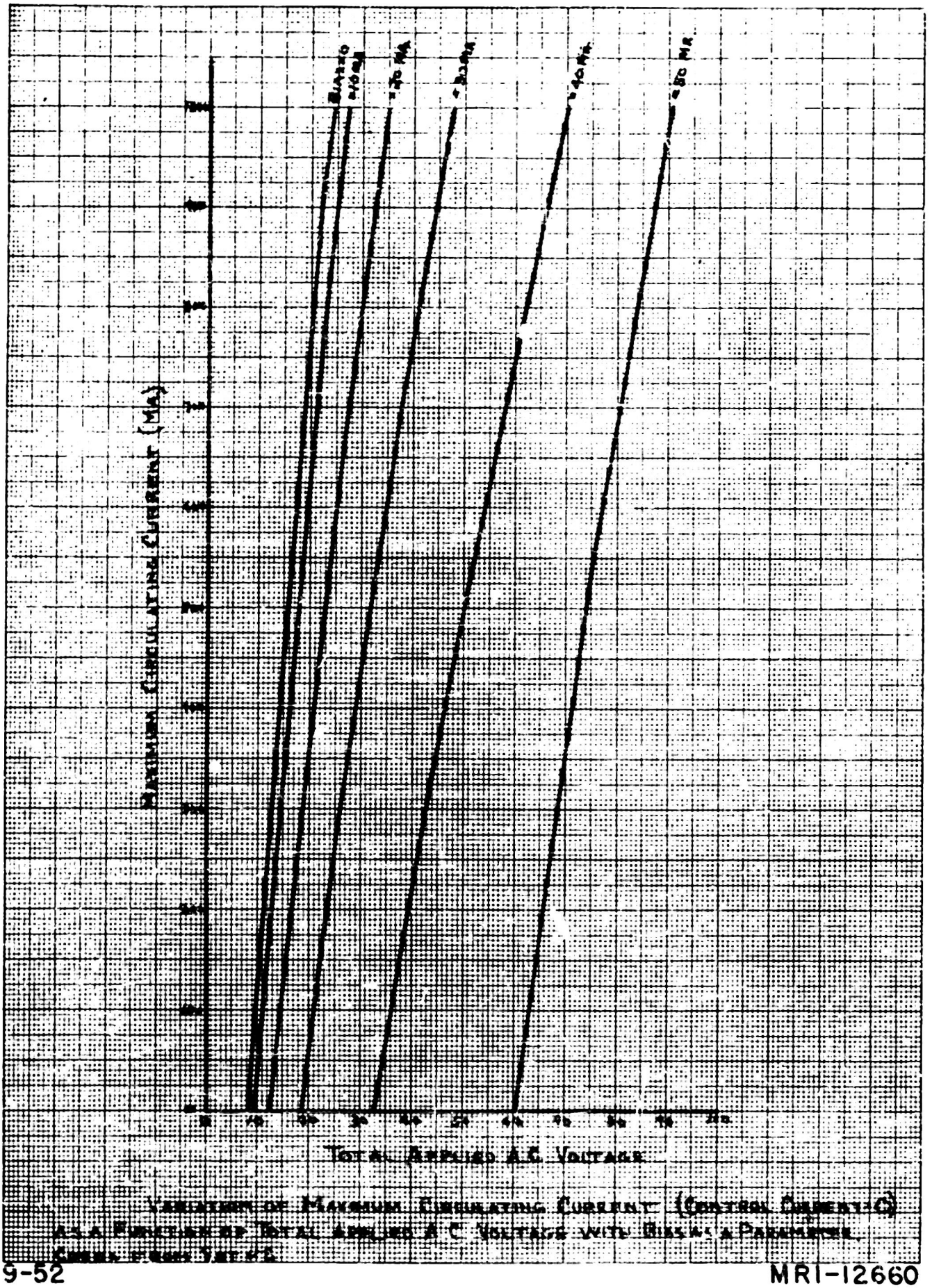

Variation of Maximum Circulating Current (Control Current=0) as a Function of Total Applied A.C. Voltage with Bias as a Parameter.
Circuit Figure 3.2-12

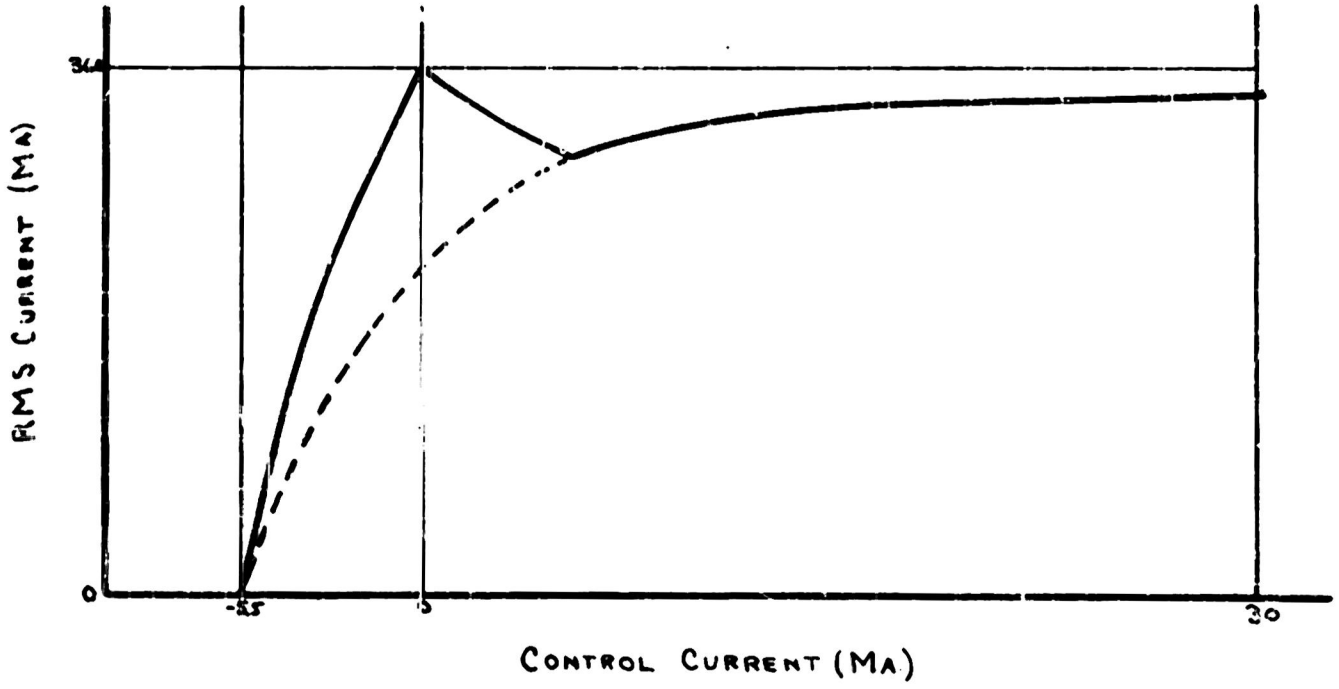

Current in one Doubler of a Push-Pull Current Subtraction Circuit, Showing the Typical Sharp Peak to be Expected at Zero Control Current. (Data Obtained From Cores of Set #2 for Typical Circuit Adjustment.)

DIEHL NO. S.S. FPE25-33-1 ALTERNATING CURRENT LOW INERTIA SERVO MOTOR

TYPICAL MANUFACTURER'S DATA FOR SERVO MOTORS

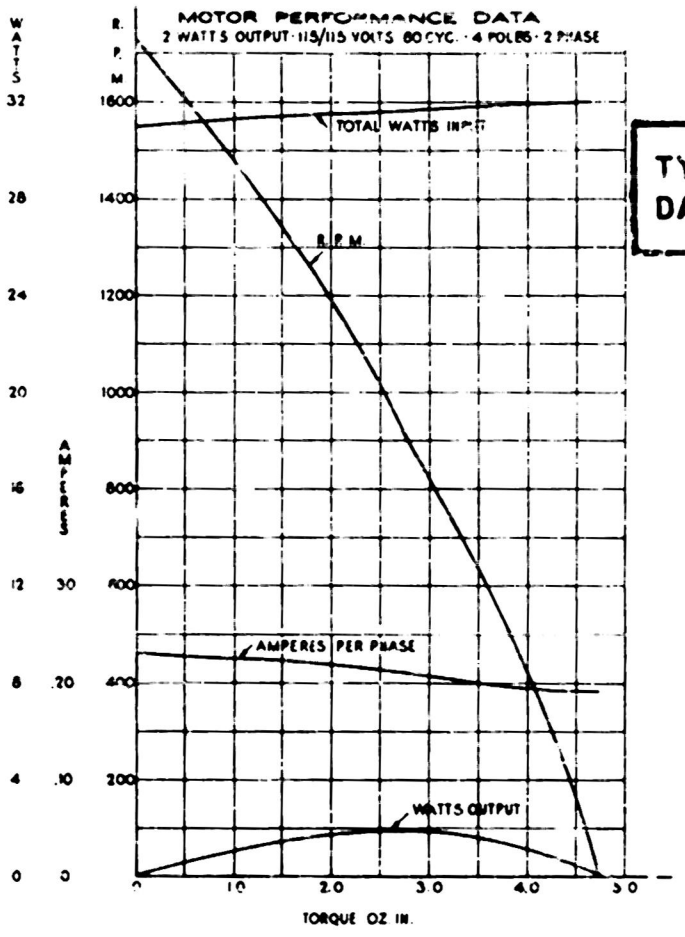

ID 4022

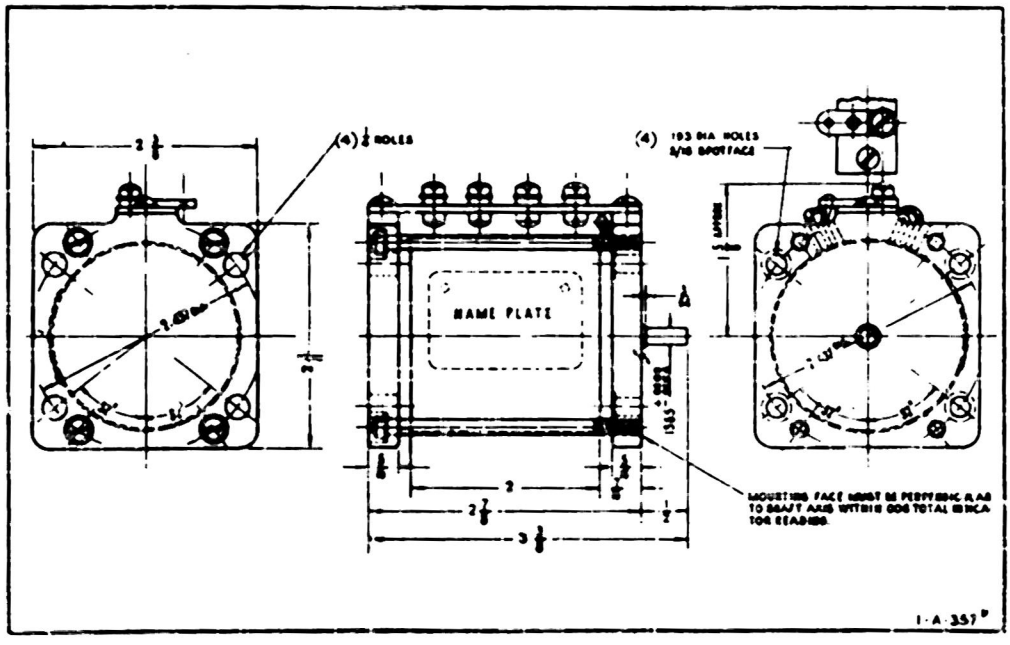

1-A-357

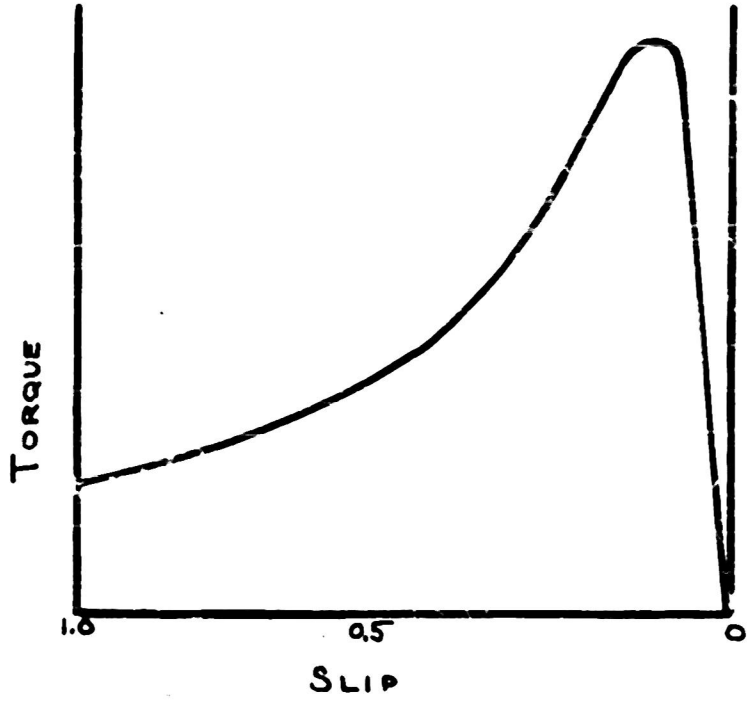

SPEED-TORQUE CHARACTERISTIC FOR THE USUAL POLYPHASE INDUCTION MOTOR

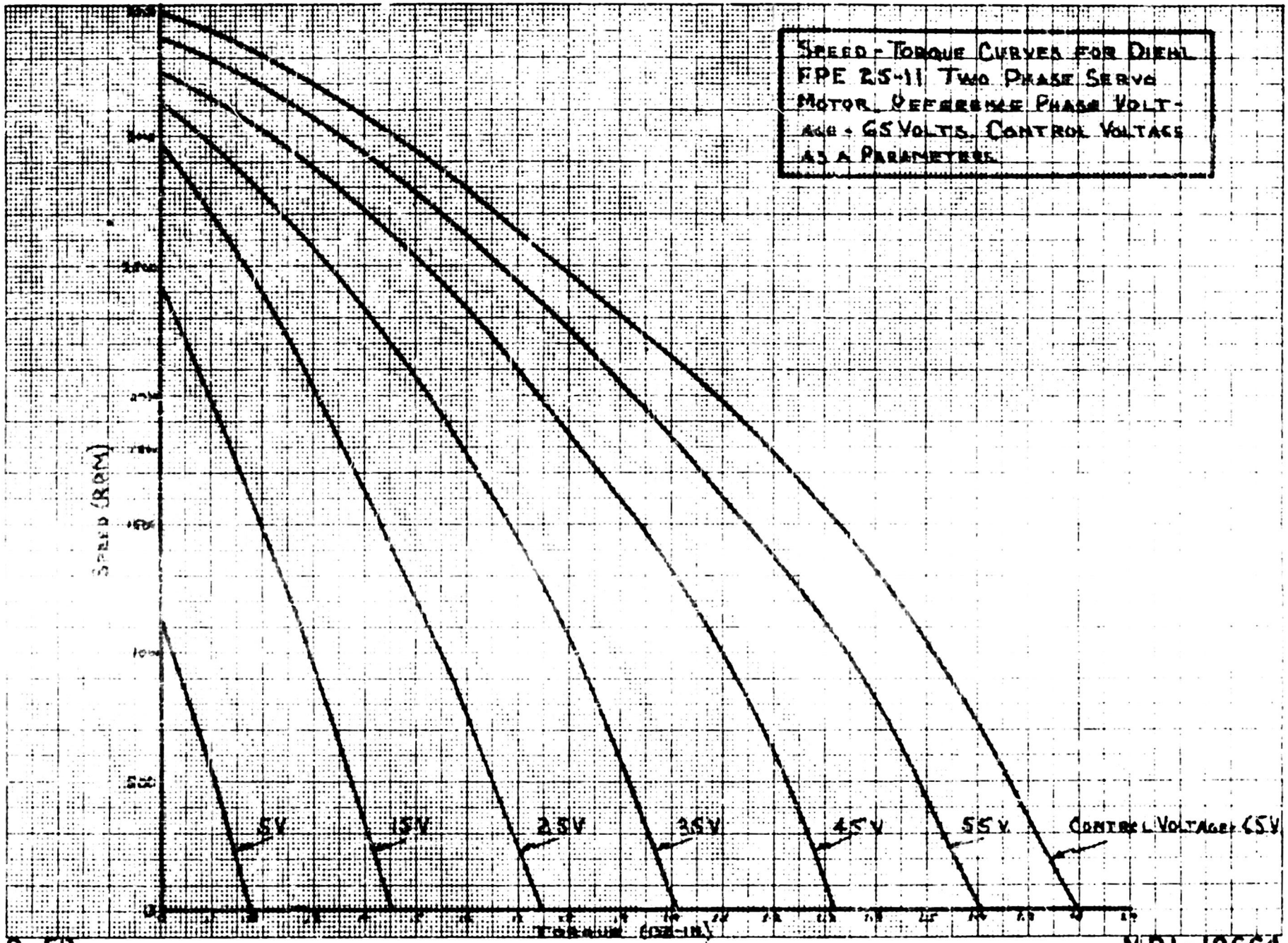

SPEED - TORQUE CURVES FOR DIEHL FPE 2.5-11 TWO PHASE SERVO MOTOR. REFERENCE PHASE VOLTAGE = 65 VOLTS. CONTROL VOLTAGE AS A PARAMETER.

MRI-12664

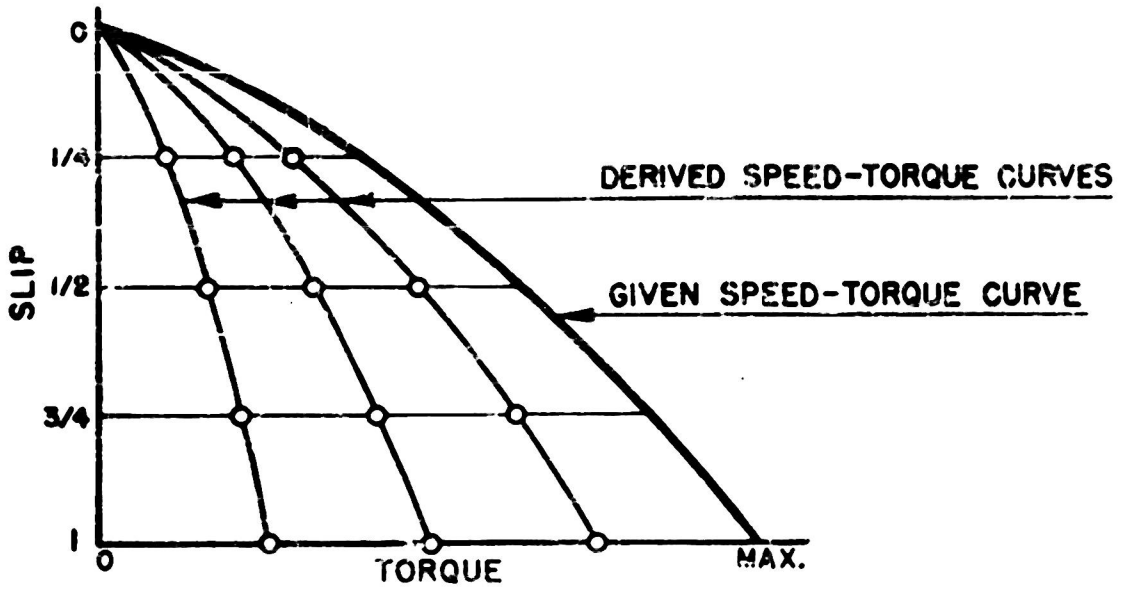

(a)-DERIVATION OF A FAMILY OF SPEED-TORQUE CURVES FROM A BALANCED VOLTAGE SPEED-TORQUE CURVE USING ONLY ASSUMPTION (2)

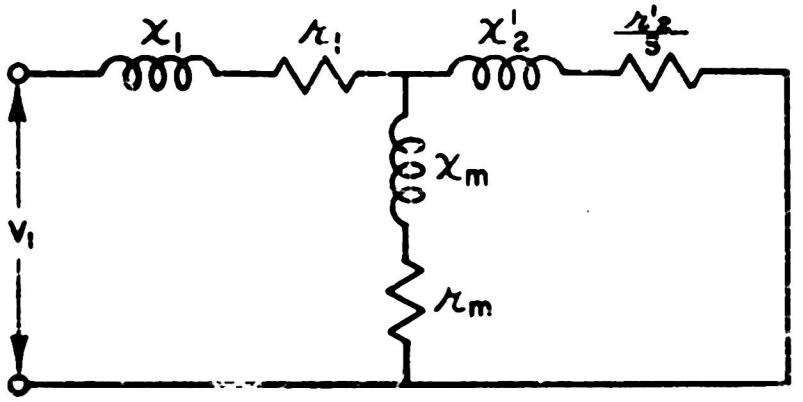

(b)-EQUIVALENT CIRCUIT OF THE POLYPHASE INDUCTION MOTOR

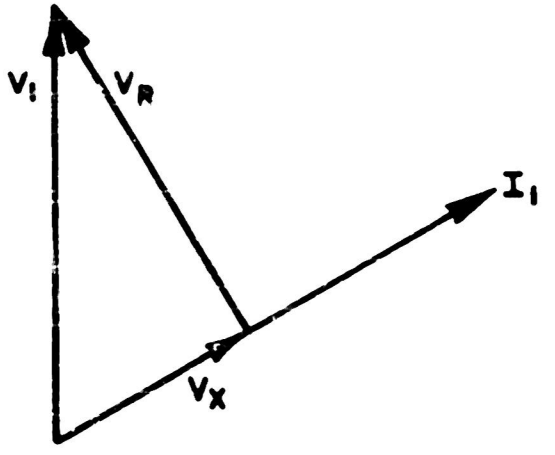

(c)-RESOLVING THE APPLIED MOTOR VOLTAGE INTO A REAL AND REACTIVE COMPONENT

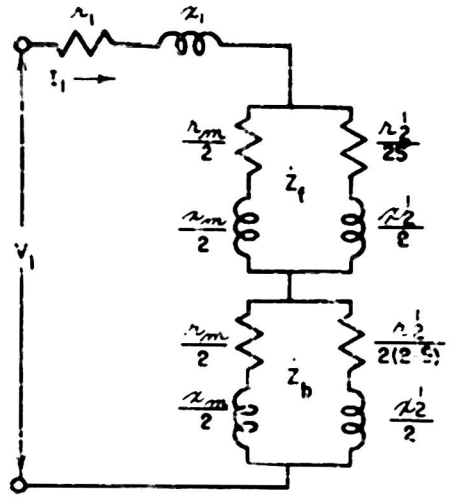

EQUIVALENT CIRCUIT OF ONE PHASE OF A TWO PHASE MOTOR

(a)

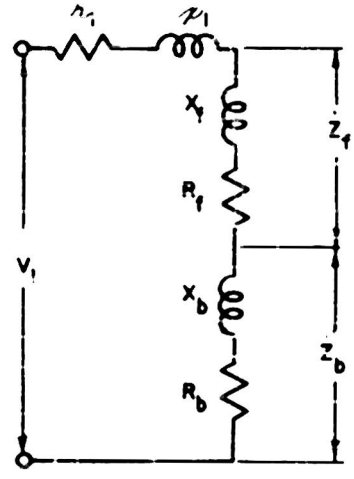

REDUCED EQUIVALENT CIRCUIT OF A SINGLE PHASE OF A TWO PHASE MOTOR

(b)

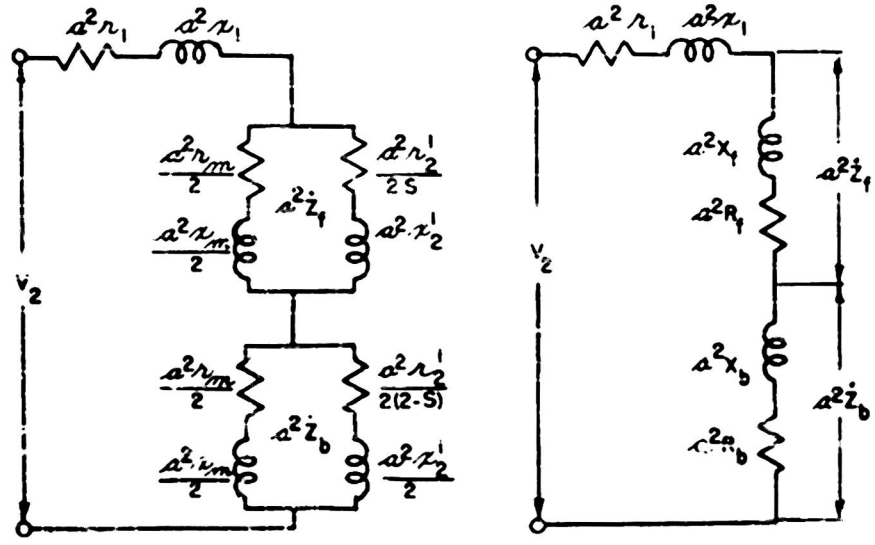

EQUIVALENT CIRCUIT OF THE SECOND PHASE OF A TWO PHASE SERVO MOTOR REFERRED TO THE FIRST (a USUALLY = 1)

(c)

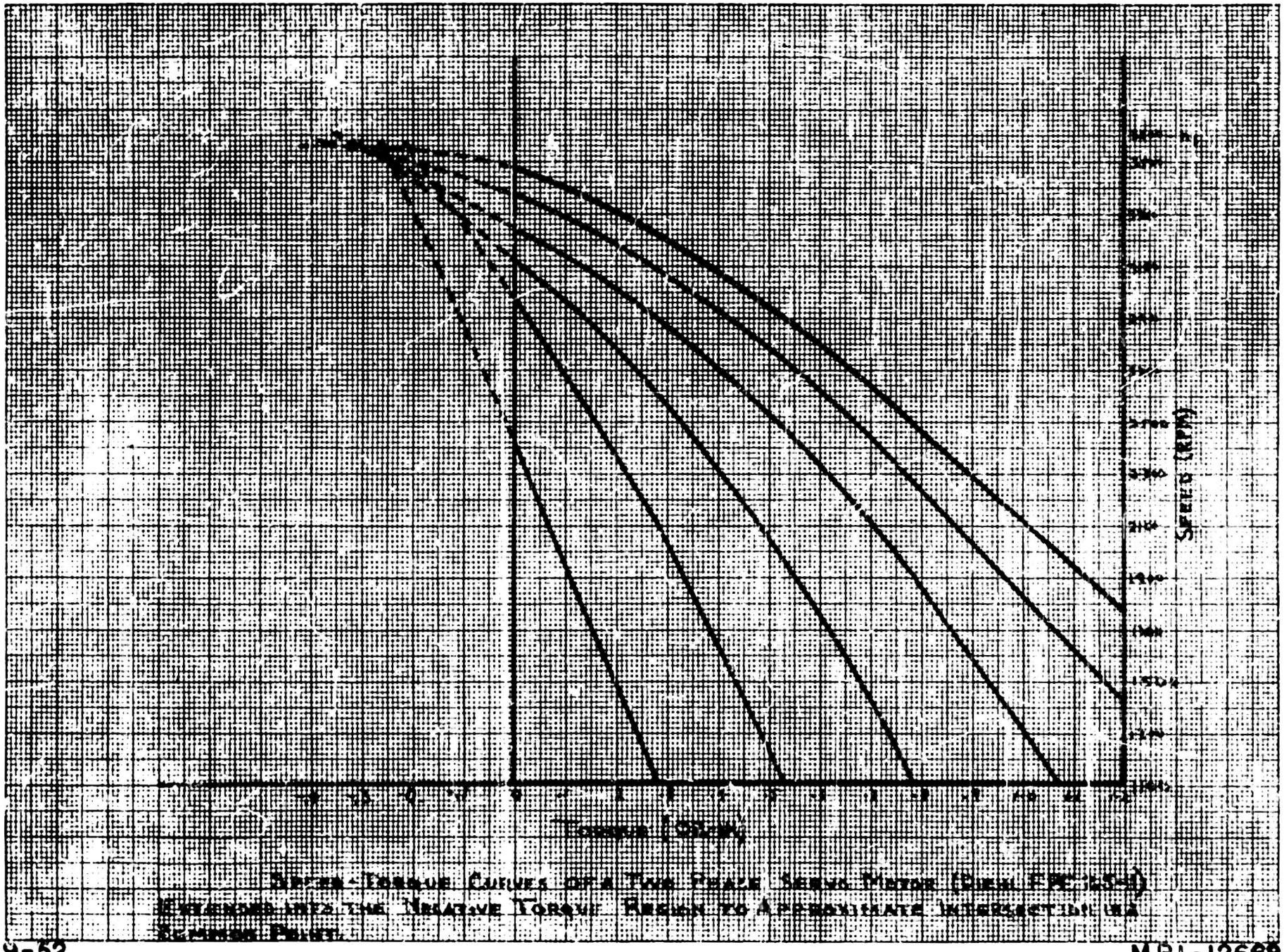

SPEED-TORQUE CURVES OF A TWO PHASE SERVO MOTOR (DWG. FPC-1503) EXTENDED INTO THE NEGATIVE TORQUE REGION TO APPROXIMATE INTERSECTION WITH SERVICE POINT.

COMPARISON CHART FOR THE VACUUM TUBE AND SERVO MOTOR

VACUUM TUBE	MOTOR
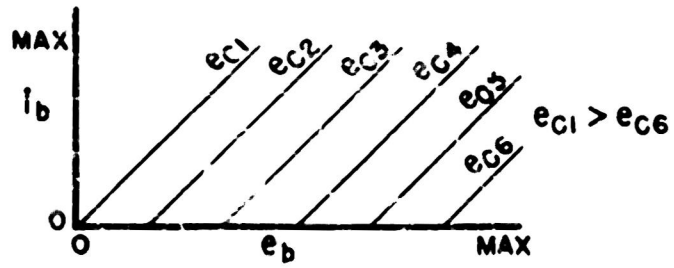 PLATE CHARACTERISTICS	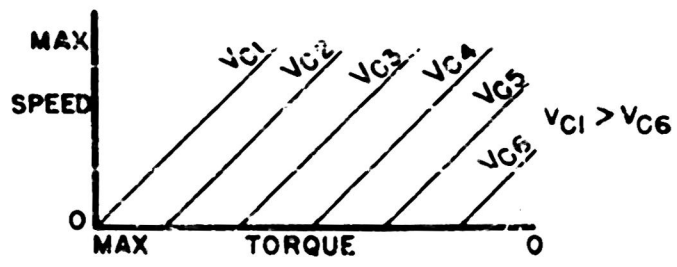 SPEED–TORQUE CHARACTERISTICS

i_b	S
e_b	T
e_c	V_c

ANALOGOUS QUANTITIES

$g_m = \left.\frac{\partial i_b}{\partial e_c}\right\|_{e_b = \text{CONST.}}$	$g_{m_m} = \left.\frac{\partial S}{\partial V}\right\|_{T = \text{CONST.}}$
$r_p = \left.\frac{\partial e_b}{\partial i_b}\right\|_{e_c = \text{CONST.}}$	$r_{p_m} = \left.\frac{\partial T}{\partial S}\right\|_{V = \text{CONST.}}$
$\mu = \left.\frac{\partial e_b}{\partial e_c}\right\|_{i_b = \text{CONST.}}$	$\mu_m = \left.\frac{\partial T}{\partial V}\right\|_{S = \text{CONST.}}$

ANALOGOUS DERIVATIVE DESCRIPTIONS

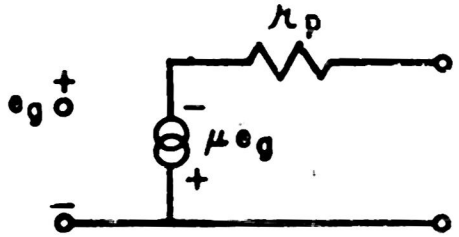 VOLTAGE GENERATOR EQUIVALENT CIRCUIT	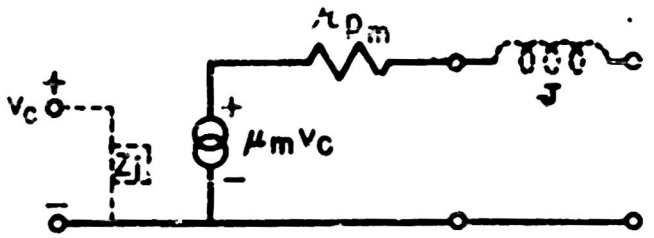 TORQUE GENERATOR EQUIVALENT CIRCUIT
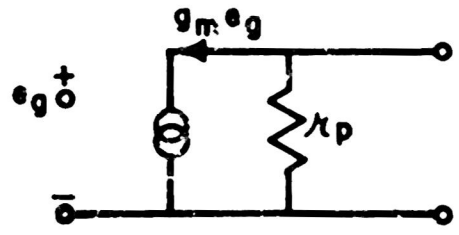 CURRENT GENERATOR EQUIVALENT CIRCUIT	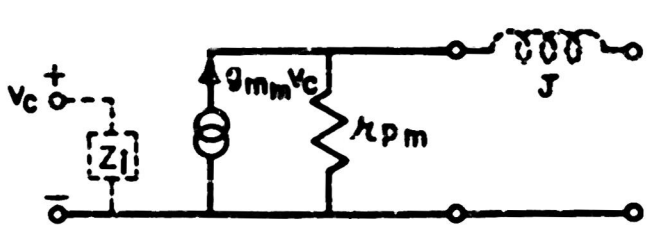 SPEED GENERATOR EQUIVALENT CIRCUIT

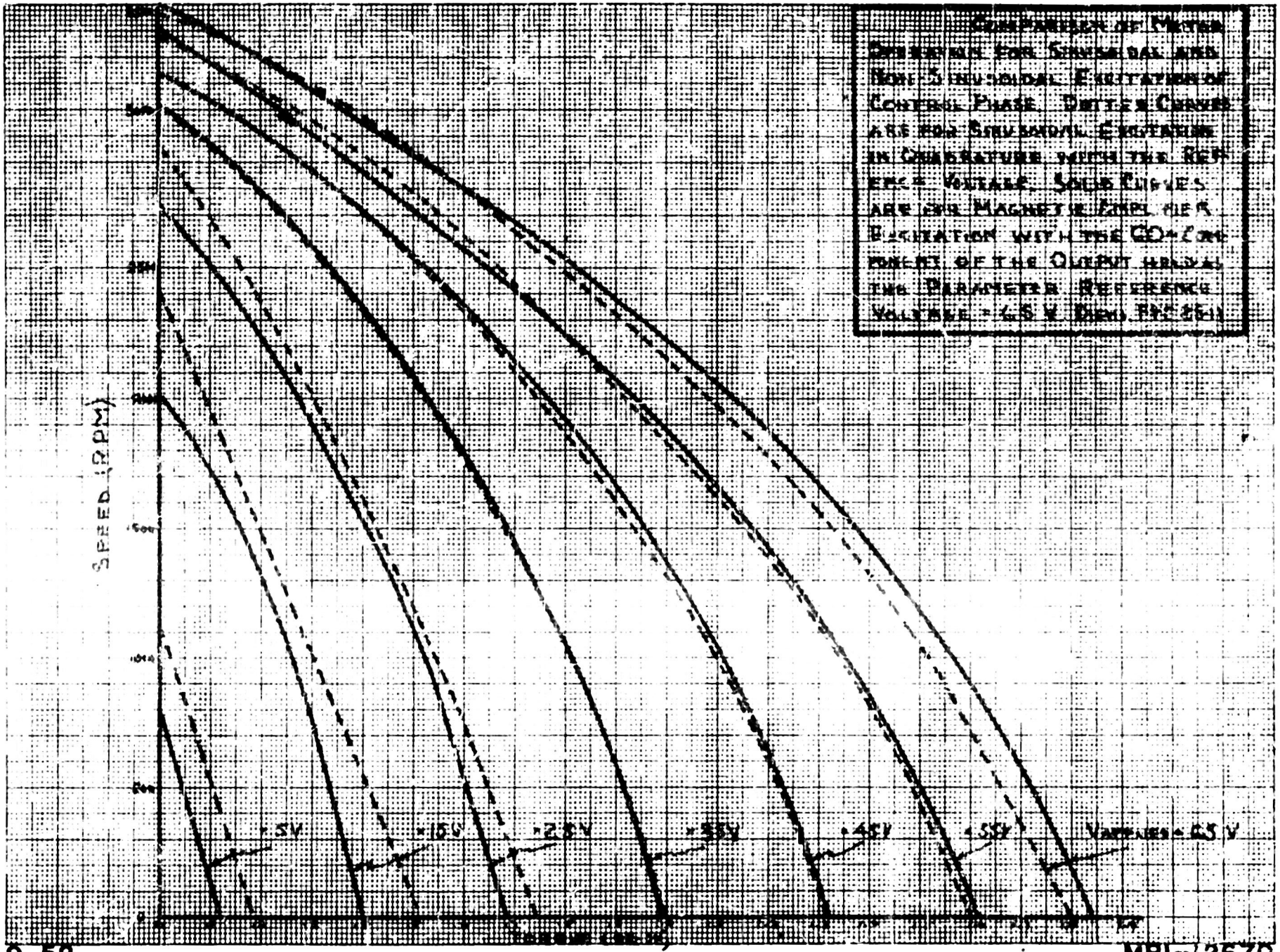

Comparison of Motor Operation for Sinusoidal and Non-Sinusoidal Excitation of Control Phase. Dotted Curves are for Sinusoidal Excitation in Quadrature with the Reference Voltage. Solid Curves are for Magnetic Amplifier Excitation with the 60-Cycle Component of the Output Signal. The Parameter Reference Voltage -6.5 V. Rem. Fig. 26-11

Sequence of output voltage waveshapes from full output voltage in one phase to full output voltage in the opposite phase. The mechanism of phase reversal is apparent. Figures (a) and (h) are the maximum possible outputs; sequence is from (a) through (h) as a function of control current.

MRI-92672

9852

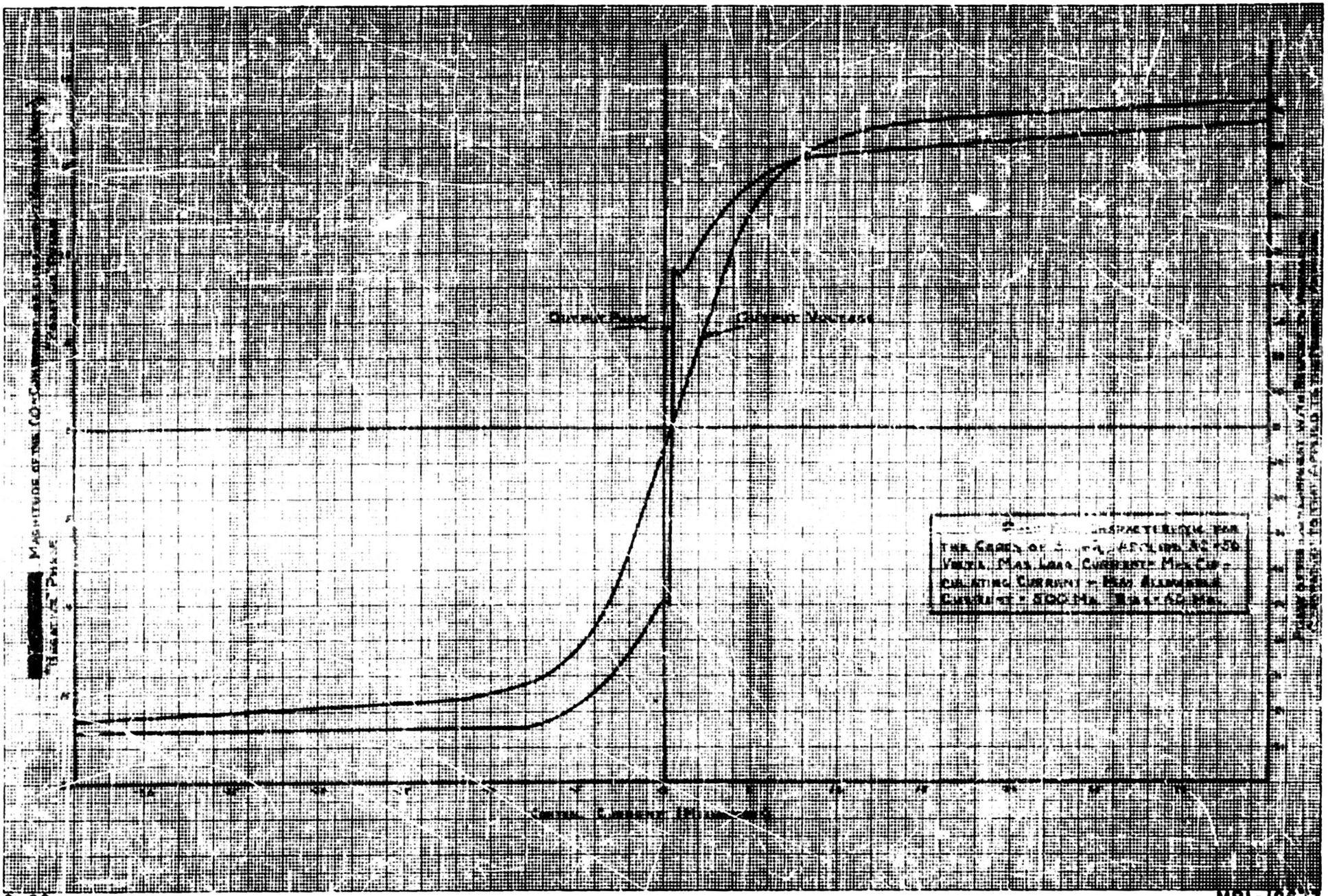

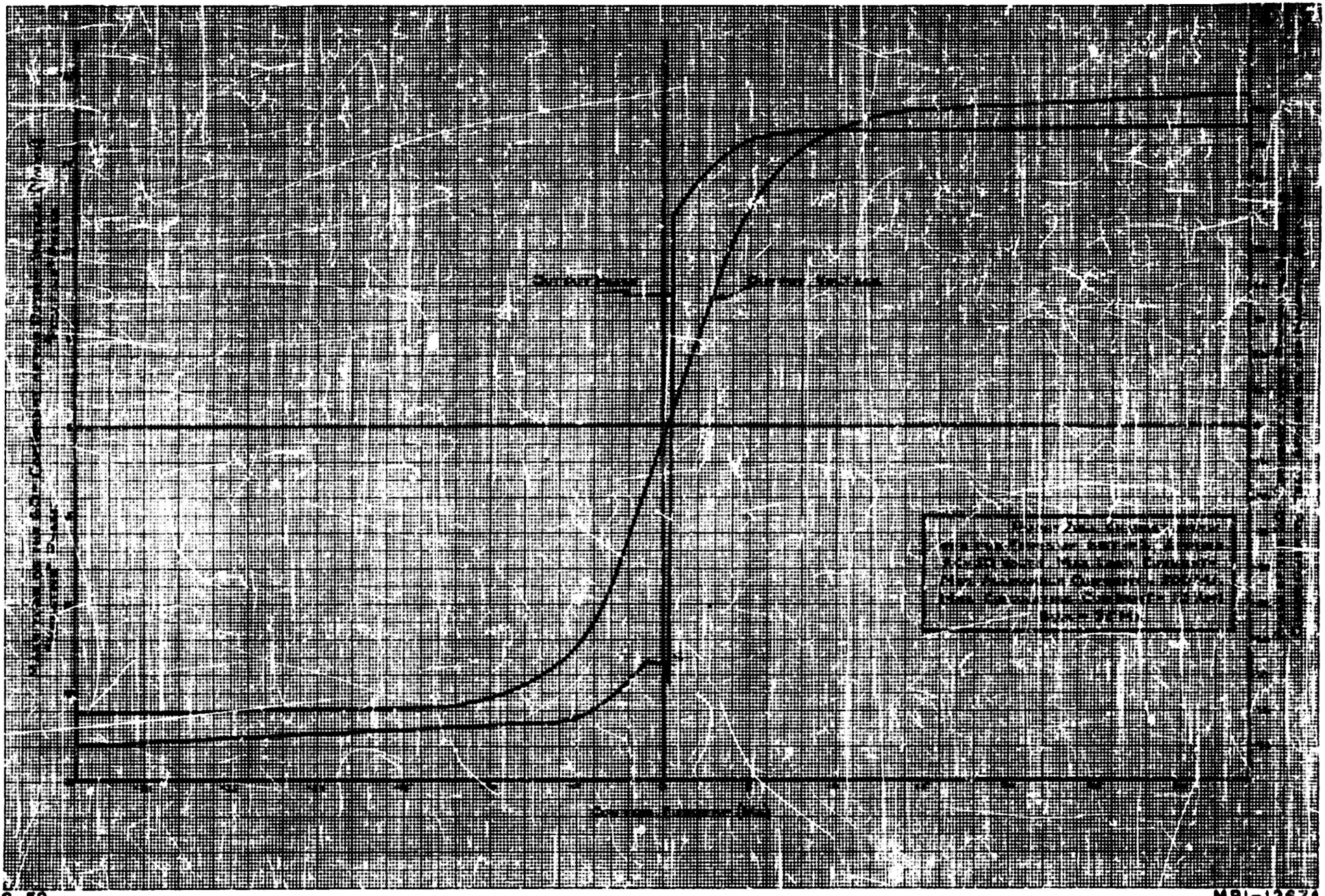

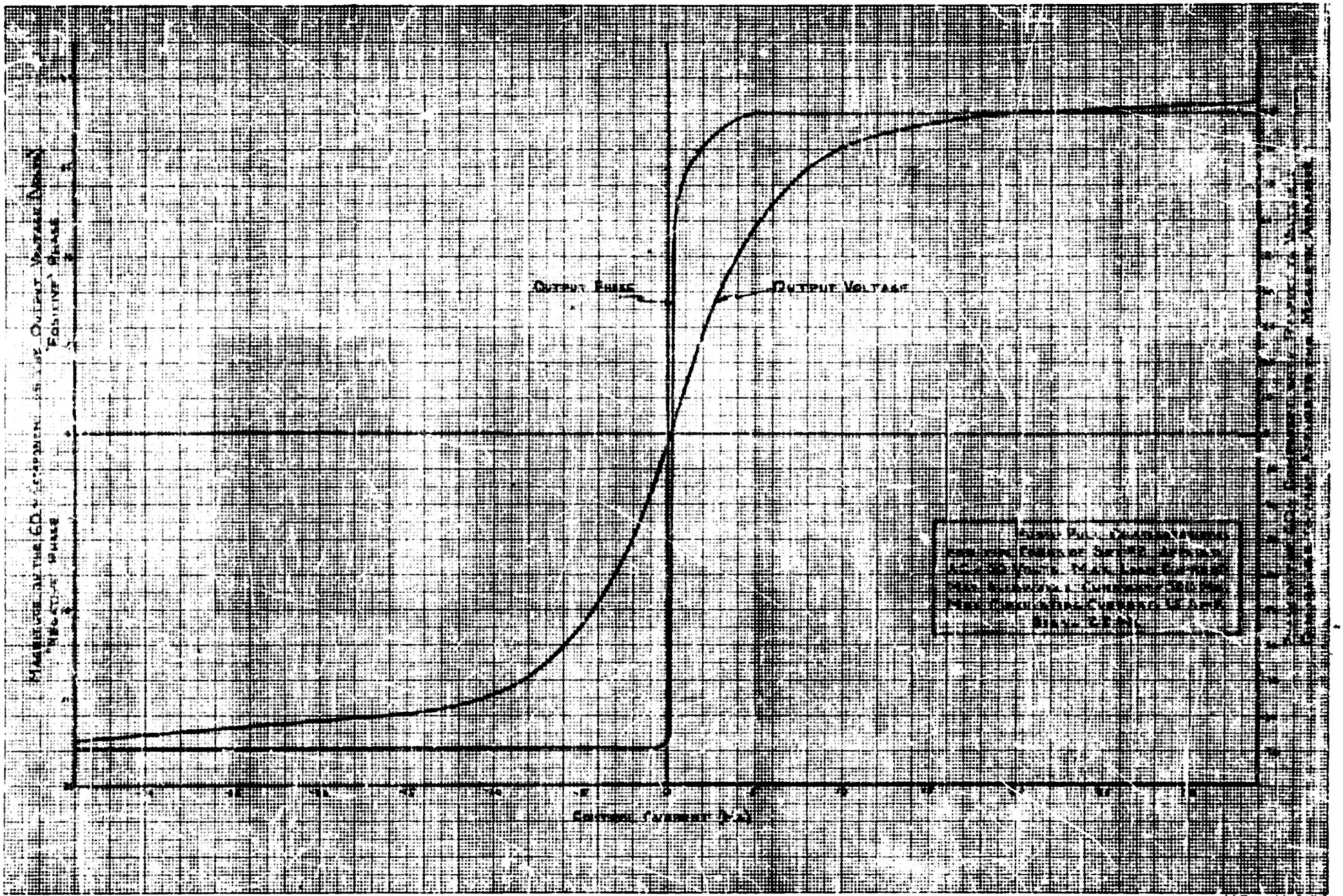

9-52

MRI-12675

Output Current

Output Voltage

Single Doubler

Output Voltage

Output Current

Push-Pull Doublers

Waveshapes of Output Voltage and Current With a Resistive Load for a Single Doubler and for the Push-Pull Connection.

(a)

Output Current

Output Voltage

Single Doubler

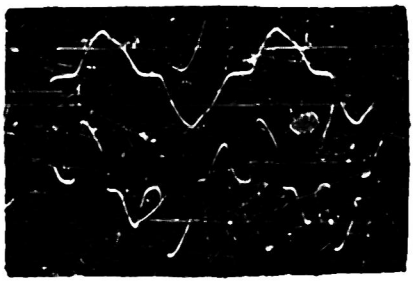

Output Current

Output Voltage

Push-Pull Doublers

Waveshapes of Output Voltage and Current With an Inductive Load for a Single Doubler and for the Push-Pull Connection.

(b)

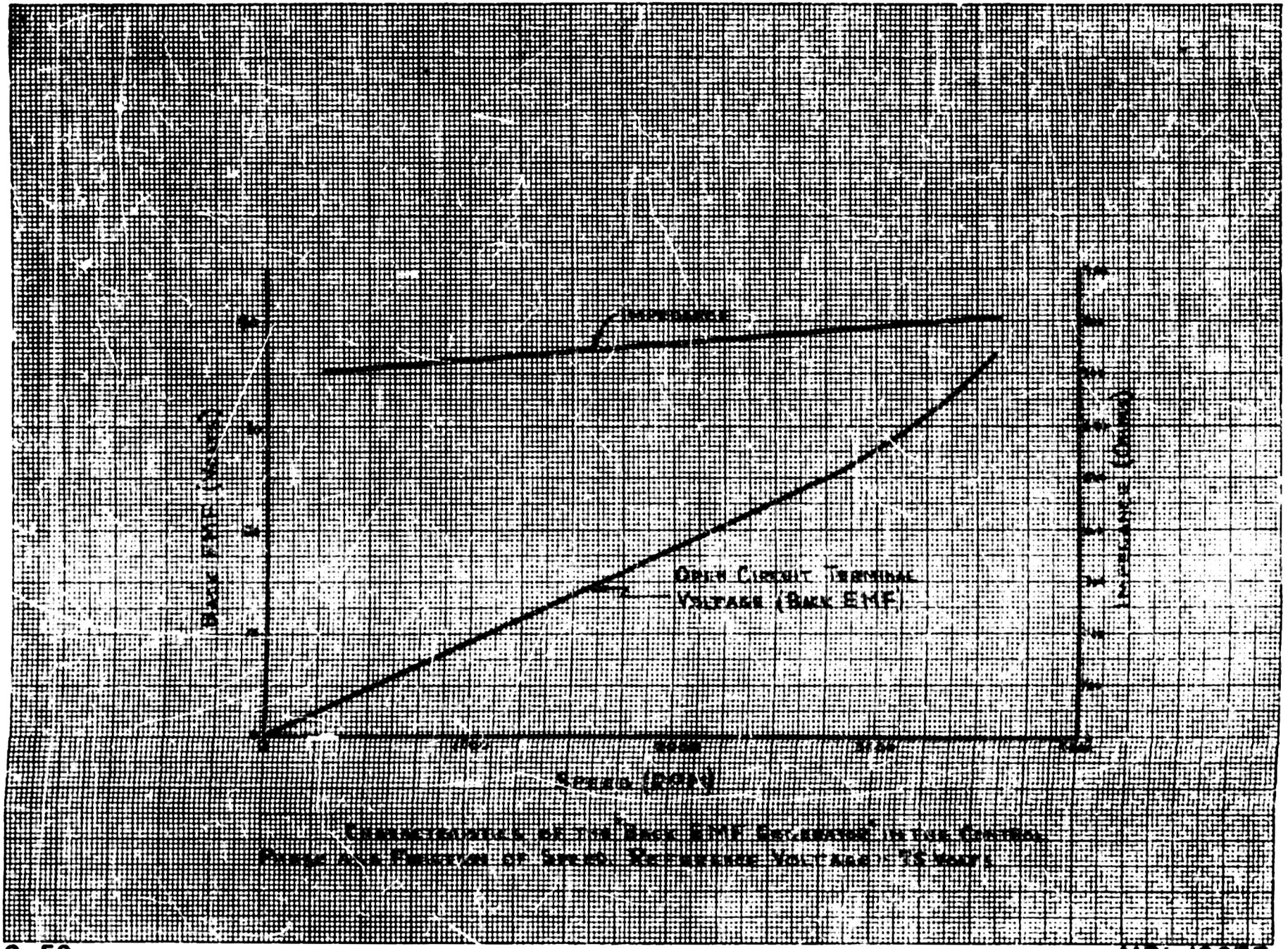

Characteristics of the Back EMF Regulator in the Control Panel as a Function of Speed. Reference Voltage = 75 Volts

MRI-12677

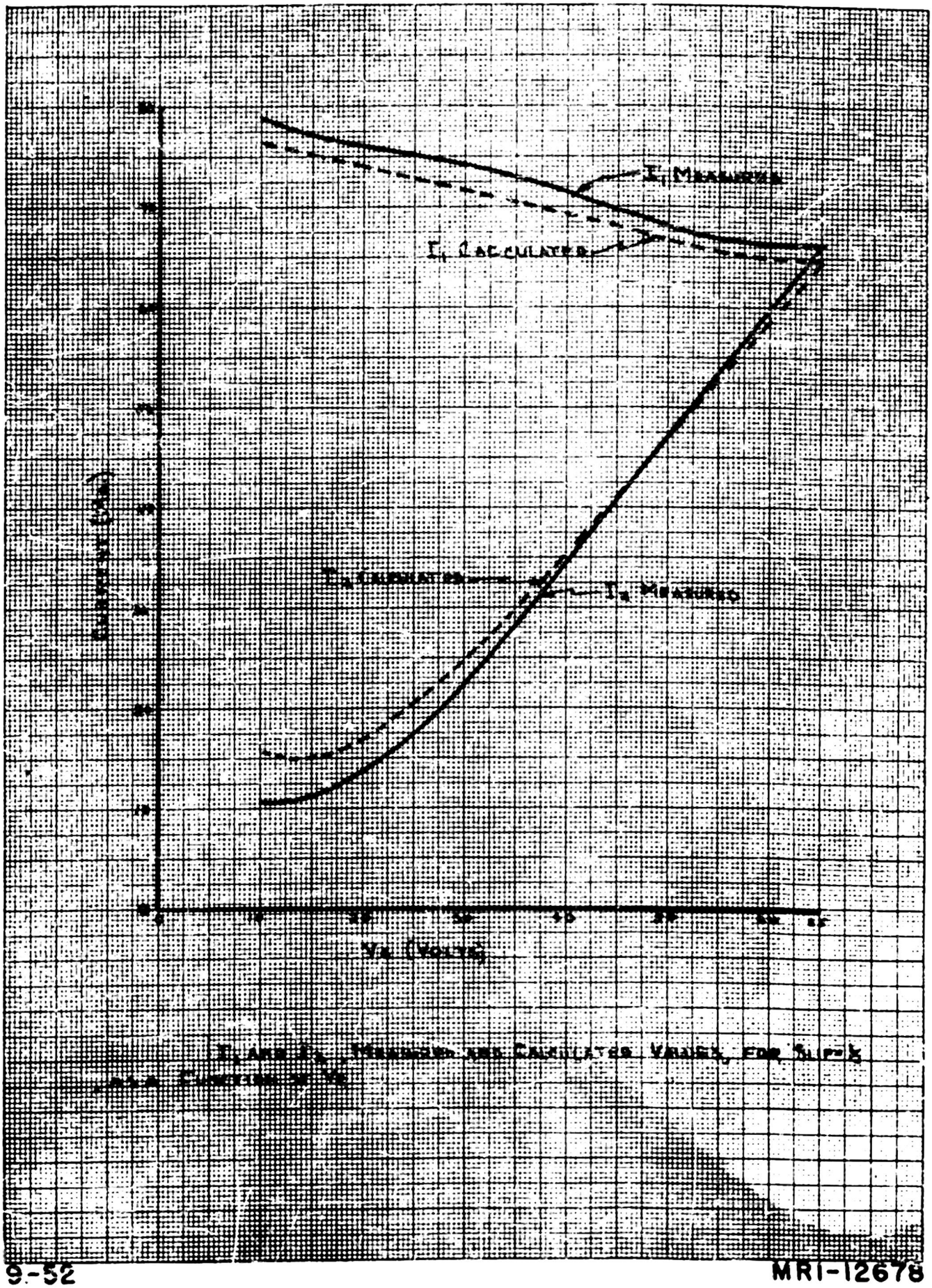

I_1 and I_2, Measured and Calculated Values, for Slip = s.s.s. Function of V_2